Sensitivity of groundwater levels to low-frequency climate variability in a large watershed

Lisa Baulon, Manuel Fossa, Nicolas Massei, Nicolas Flipo, Nicolas Gallois, Matthieu Fournier, Bastien Dieppois, L. Danaila, Delphine Allier, Hélène Bessiere

Science of the Total Environment 957 (2024) 177636

Contents lists available at ScienceDirect

Science of the Total Environment

journal homepage: www.elsevier.com/locate/scitotenv

Sensitivity of groundwater levels to low-frequency climate variability in a large watershed

Lisa Baulon [a,b,*], Manuel Fossa [b], Nicolas Massei [b], Nicolas Flipo [c], Nicolas Gallois [c], Matthieu Fournier [b], Bastien Dieppois [d], Luminita Danaila [b], Delphine Allier [a], Hélène Bessiere [a]

[a] BRGM, 3 av. C. Guillemin, 45060 Cedex 02 Orleans, France
[b] Normandie Univ, UNIROUEN, UNICAEN, CNRS, M2C, 76000 Rouen, France
[c] Mines Paris, PSL University, Centre for Geosciences and Geoengineering, Fontainebleau, France
[d] Centre for Agroecology, Water and Resilience (CAWR), Coventry University, UK

HIGHLIGHTS

- Scenarios of changing low-frequency climate variability were developed.
- Influence on groundwater levels over the Paris Basin was assessed.
- The physics-based model CaWaQS was used for assessing this influence.
- Groundwater levels showed clear sensitivity to changes in climate variability.
- Mean, low, and high groundwater levels were significantly affected.

GRAPHICAL ABSTRACT

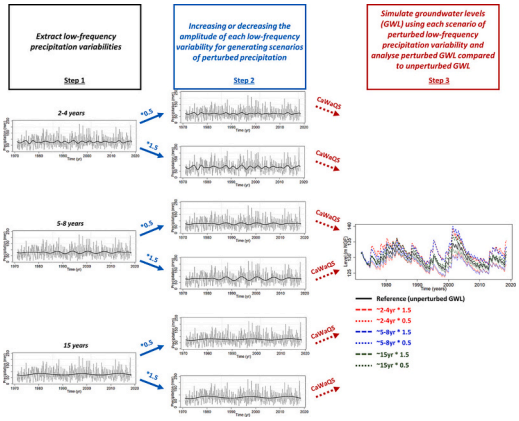

ARTICLE INFO

Editor: Christian Herrera

Keywords:
Groundwater levels
Paris Basin
Physically-based modeling
Low-frequency climate variability

ABSTRACT

Groundwater level (GWL) can vary over a wide range of timescales. Previous studies highlighted that low-frequency variability (interannual (2–8 years) to decadal (>10 years)) originating from large-scale climate variability, represents a significant part of GWL variance. It remains an open question, however, how GWL, including extremes, may respond to changes in large-scale climate forcing, affecting precipitation variability. Focusing on the Seine River basin, this study therefore aims to assess how GWLs respond to changes in inter-annual to decadal climate variability.

We implemented an empirical numerical approach, which enables an assessment of the GWL sensitivity to changes in precipitation variability over a range of timescales (up to decadal), using the Seine hydrosystem as a case study. The approach consists in: i) identifying and modifying the spectral content of precipitation in the low-frequency range; ii) using these perturbed precipitation fields as input in the physically-based hydrological/hydrogeological CaWaQS model for the Seine River basin to simulate the corresponding GWL response; iii)

* Corresponding author at: BRGM, 3 av. C. Guillemin, 45060 Cedex 02 Orleans, France.
E-mail address: l.baulon@brgm.fr (L. Baulon).

https://doi.org/10.1016/j.scitotenv.2024.177636
Received 19 July 2024; Received in revised form 14 November 2024; Accepted 17 November 2024

comparing the spectral content, mean, variance and extremes of perturbed GWLs with reference (i.e. unperturbed) GWLs. Two interannual (2–4 yr and 5–8 yr) and one decadal (15 yr) timescales were modified individually by either increasing or decreasing their amplitude by 50 %. This led to six scenarios of perturbed low-frequency precipitation variability, which were subsequently used as CaWaQS inputs to assess the GWL response.

Results indicated increased (decreased) GWL up to 5 m when low-frequency precipitation variability increased (decreased) by 50 %. This led to an increased occurrence of groundwater floods (droughts) with increased severity and decreased occurrence of groundwater droughts (floods) with decreased severity, respectively. These results indicate: i) how using biased climate data, in terms of low-frequency variability, leads to large deviations in the GWL simulation, ii) to what extent potential changes in low-frequency climate variability may affect future GWL, and particularly drought and flood occurrence and severity.

1. Introduction

Climate change is significantly affecting long-term trends in water resources at the global scale. Internal climate variations have been found to modulate these trends at the regional scale (Boé and Habets, 2014; Sidibe et al., 2019; Liesch and Wunsch, 2019; Bonnet et al., 2020). For water resources, internal modes of climate variability such as the North-Atlantic Oscillation (NAO) or the El Nino-Southern Oscillation (ENSO) often explain the succession of dry and wet years to which human activities are particularly vulnerable (Habets et al., 2010; Blöschl et al., 2019; Maréchal and Rouillard, 2020). Linkages between these modes and regional hydroclimate (precipitation, temperature, streamflow) in NW Europe and France have been extensively studied, and much of this work highlighted that such links were occurring across several main time scales (Massei et al., 2010; Dieppois et al., 2013, 2016; Boé and Habets, 2014; Fossa et al., 2021; Lorenzo-Lacruz et al., 2022): interannual (2-4 yr and 5-8 yr), decadal (15-yr), and multidecadal (30-yr and 60-yr). In northwestern Europe, the NAO was described as a significant driver of such temporal signatures in precipitation, streamflow and groundwater levels (Massei et al., 2007, 2010; Holman et al., 2011; Massei and Fournier, 2012; Rust et al., 2022; Lorenzo-Lacruz et al., 2022). However, in metropolitan France, only interannual ~5-8 yr and decadal ~15 yr variability of the NAO were found to be directly related to hydrology over the same timescales (Massei et al., 2010), which may explain why linear correlation has failed to detect any link between hydrology and the NAO index (e.g. Giuntoli et al., 2013). Other teleconnection patterns, such as the Scandinavia pattern or the East Atlantic pattern, may also display remarkable relationships with interannual and decadal hydrological variability (Neves et al., 2019; Liesch and Wunsch, 2019; Lorenzo-Lacruz et al., 2022).

For groundwater level (GWL), such timescales can explain a significant part of long-term variations, depending on the physical properties of aquifers which behave as low-pass filters (Slimani et al., 2009; El Janyani et al., 2012; Velasco et al., 2017; Rust et al., 2018; Schuite et al., 2019). As underlined in Baulon et al. (2022a, 2022b) and more recently recalled in Chidepudi et al. (2023, 2024a), the GWLs of French aquifers may have reactive, inertial, or so-called "mixed" or "combined" temporal behavior. Inertial water tables are poorly reactive to aquifer recharge and have a slow discharge, displaying variations over interannual to decadal timescales. Conversely, reactive water tables have a quick response to recharge and rapid discharge, displaying variations over annual and even sub-annual timescales. Mixed-type water tables lie in between, displaying variations over annual and sub-annual scales superimposed to interannual and decadal variability. The GWLs of inertial and mixed water tables, which are significantly affected by interannual to decadal variability (also called "low-frequency variability"), exhibit groundwater droughts and floods that are known to be largely controlled by large-scale climate variations on the same timescales, as shown by Baulon et al. (2022b). Groundwater resource variations can then very often display such low-frequency fluctuations originating from climate variability, which might be associated with sustained multi-year flood or drought-rich periods as described in Blöschl et al. (2019) as an unsolved hydrological problem. As a result, the first main issue to address is: How low-frequency climate variability will be affected by climate change and how those changes will impact water resources.

Moreover, the influence of climate change on groundwater (quantity) has not been clearly established using historical measurements (Douville et al., 2021) as there are many limiting parameters that continue to constrain the understanding of the impacts of climate change on groundwater: the spatio-temporal coverage of groundwater monitoring networks, the availability of abstraction data, or the modeling of recharge processes (Douville et al., 2021). A recent study emphasized that 80 % of Euro-Mediterranean regions showed declining GWLs over the 2003–2020 period (GRACE data; Xanke and Liesch, 2022). It is however difficult to disentangle the respective impacts of climate change (decreasing recharge rates) and abstraction constraints in these trends. Xanke and Liesch (2022) also indicate that climatic influences appear to play a minor role in these trends in most of the Euro-Mediterranean area, since recharge trends are generally not significant. Based on observation data, another recent study indicated that southwestern Europe (France, Spain, Portugal, Italy) did not show major changes in GWLs over the 1985–2014 period (Chávez García Silva et al., 2024). Water tables displaying stable levels are located in temperate climate zones (the case of the Seine River basin) with year-round high precipitation. Water tables in southwestern Europe, where levels are nevertheless decreasing, are often exposed to abstraction for agricultural uses (the case of semi-arid regions also exposed to prolonged soil moisture loss in summer) or for urban areas (the case of temperate regions).

Furthermore, the link between GWL trends and climate change is all the more difficult to determine for aquifers with high interannual variability (such as the Seine River basin; Baulon et al., 2022a). Interannual variability, linked to internal climate variability, is responsible for accentuating, attenuating, or even masking trends linked to climate change.

The impact of climate change on GWLs by 2100 is, however, more clearly established. Germany, for example, is expected to experience a significant decrease in GWLs by 2100, particularly under RCP8.5 (Wunsch et al., 2022). Chidepudi et al. (2024b) also identified such decreasing trends for the water tables of northern France, which are also accentuated under the RCP8.5 scenario. The result differs from that of the study conducted by Vergnes et al. (2023), which indicated an increase in GWLs for northern France. However, the methodology of the two studies differed, since Chidepudi et al. (2024b), like Wunsch et al. (2022), studied trends in future projections to the 2100 horizon, whereas Vergnes et al. (2023) compared projections for the 2070–2099 period (far future) with the historical period 1976–2005 (reference period). Chidepudi et al. (2024b) also estimated the relative difference in GWLs between the far future and the historical periods, and also identified projected annual average levels higher than historical levels, for all emission scenarios, which corroborates the results of Vergnes et al. (2023). The same methodology was replicated by Sauquet et al. (2024) on groundwater recharge and levels in France. While there is a consensus between the different simulations for recharge, with projected recharge in the far future higher than historical recharge in northern France under the RCP8.5 scenario, there is no consensus between the different simulations for GWLs.

However, one of the limitations of these studies comes from the inability of climate models (used for generating climate projections) to correctly represent the amplitude of internal (stochastic) climate variability, which consequently accounts for a significant part of the uncertainty in hydroclimatic projections, particularly for groundwater. Such uncertainties therefore may not be properly handled in groundwater projections. For instance, Terray and Boé (2013) estimated that uncertainties related to internal climate variability in precipitation projections over France in the middle of the 21st century may be as large as uncertainties due to climate models. More recently, Boé (2020) showed that interannual variability is overestimated by around three-quarters of the CMIP6 models in winter and spring over the Seine River basin. In summer and autumn, around half and two-thirds of the models are respectively consistent with observations (Boé, 2020).

In addition, the studies addressing the impact of climate change on GWL focus very little on the changes in low-frequency climate variability that climate change may cause, but rather on trends. There is therefore a lack of knowledge about how changes in the amplitude of low-frequency climate variability in the coming decades could affect GWL. In addition, the climate model outputs (i.e., projections) used in these studies do not cover all the possible scenarios of changes in climate variability.

In this paper, we therefore present a preliminary approach to evaluate how GWLs in a large hydrosystem would be sensitive to different amplitudes of climate low-frequency variability. This research was guided by two major scientific questions:

- How may groundwater resources respond to changes (natural or climate change-related) in low-frequency climate variability?
- To what extent is groundwater simulation biased by the improper representation of low-frequency climate variability by climate models?

In other words, the idea is to develop an approach to assess how aquifers would react to different amplitudes of low-frequency climate variability input, be they caused by improper representation in the climate models used for generating projections, or by actual changes that may occur within the next decades. The approach developed would also be useful - regardless of the issues previously mentioned – to explore scenarios of climate variability that may not be covered by the climate model outputs used for establishing the Shared Socioeconomic Pathways of the IPCC 6th assessment report (Eyring et al., 2016).

The approach focuses on developing sensitivity scenarios to assess how potential shifts in interannual to decadal climate variability could influence average GWLs, as well as extreme high and low levels, with implications for water resources. The method involves altering the amplitude of the low-frequency component of a precipitation field using a wavelet technique, and applying this modified field as input in a large-scale, physics-based hydrogeological model. The Seine River watershed was selected as a case study for three key reasons: first, its future under climate change remains uncertain (IPCC, 2021); second, a model is available that accurately represents low-frequency processes (Flipo et al., 2023); and third, the aquifers in this basin exhibit highly variable groundwater dynamics (both reactive and inertial; Baulon et al., 2022b), making it an ideal candidate for this study.

2. Demo watershed

The Seine River basin was selected as the case study, modeled using the coupled and physically-based hydrological-hydrogeological CaWaQS software (Flipo et al., 2007, 2023) to conduct numerical experiments at the regional scale. This basin is particularly well-suited for such analysis due to its surface area of 76,000 km^2, which overlies the Paris geological basin, home to the largest groundwater reservoir in Europe (Flipo et al., 2021a, 2021b).

The Seine River basin covers the sedimentary Paris Basin. Its lithology is primarily composed of carbonates (69.6 %) and sandy formations (13.6 %). As a multi-layered system, these carbonates and sandy formations are interspersed with low-permeability clay and marl units (9.1 %). The basin is also overlain by alluvial deposits (5.4 %) and carbonate-rich loess in its western and central regions (Flipo et al., 2021a). The main hydrogeological units, extending from northwest to southeast, are as follows (Fig. 1a; Flipo et al., 2021a):

- the Upper and Lower Cretaceous (in the south of Le Havre and Rouen)
- the Eocene and Oligocene calcareous and sands (around Paris), and the Miocene calcareous (further south)
- the Upper and Lower Cretaceous (around Reims, Troyes and Auxerre)
- the Upper, Middle and Lower Jurassic calcareous

The groundwater tables in the southeastern part of the Seine River basin, situated in older geological formations, are more responsive to rainfall and exhibit rapid drainage. In contrast, the groundwater tables in the central and northern regions of the basin are predominantly inertial, characterized by slow responses to precipitation and lower drainage rates (Baulon et al., 2022a, 2022b; Flipo et al., 2023).

The topography of the basin is relatively flat, with an average elevation of 300 m. The geological structure governs the arrangement of the hydrographic network, which is composed of low-gradient streams flowing from east to west and cutting through the sedimentary formations.

The total length of the river network is 27,500 km (Fig. 1b; Flipo et al., 2021a, 2021b). The main tributaries of the Seine River are the Yonne River, the Marne River, and the Oise River. The hydrological regime is pluvial/oceanic. The mean rainfall over the basin is around 800 mm/year. However, there is some spatial variability: the maximum is around 1200 mm/year along the coastal shoreline and in the Morvan mountainous range. The minimum is only 650 mm/year in the central part. The Seine discharge at the most downstream gauging station (Poses) has an average value of 485 m^3/s over the past 50 years. The discharge has even reached 2280 m^3/s in winter, and 80 m^3/s in summer (low flows are sustained by reservoirs upstream).

Rainfall in the basin does not display a distinct seasonality (Flipo et al., 2021a). Consequently, the river flow regime is driven by seasonal variations in actual evapotranspiration, leading to higher flows in winter and lower flows in summer. Streamflow is naturally and significantly supported by groundwater from aquifers, and in the middle and lower reaches of the Seine and Marne rivers, it is further regulated by upstream reservoirs.

GWLs in the Seine River basin respond across various timescales (Baulon et al., 2022b), with some aquifers dominated by low-frequency variability (inertial water tables) and others more influenced by annual variability (reactive water tables), making this basin an ideal candidate for our experiments. The diversity of aquifer types allows for a robust evaluation of how perturbations in the amplitude of the low-frequency component of rainfall affect water tables with different dynamics (inertial vs. reactive). As previously outlined, numerous previous studies have accurately identified the dominant timescales that characterize the hydrological variability (both GWL and streamflow) in the Seine watershed, which typically include interannual (~2–4 years and ~5–8 years) and decadal (~15 years) variabilities driven by large-scale climate fluctuations (Massei et al., 2010, 2017; Baulon et al., 2022b). This study focuses on analyzing the sensitivity of GWLs to these low-frequency climate variabilities.

3. Data and methodological framework

3.1. Climate and groundwater data

For this study, precipitation and temperature from SAFRAN

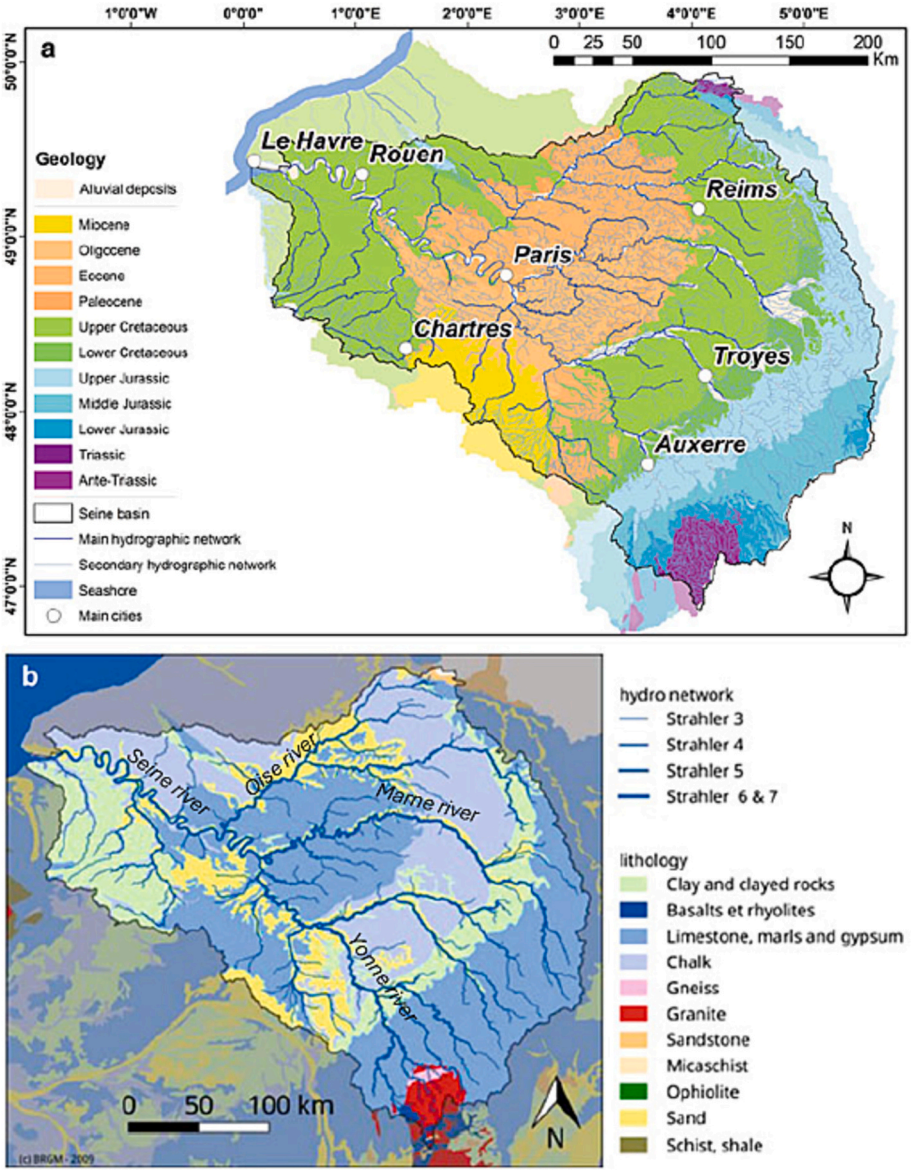

Fig. 1. (a) Geological structure of the Seine basin. (b) Lithology of the Seine basin. (Modified from Flipo et al., 2021a).

reanalysis (Système d'Analyse Fournissant des Renseignements Adaptés à la Nivologie) over the Seine River Basin for the 1970–2018 period were used as input to the CaWaQS model. This reanalysis provides daily data on an 8 × 8 km grid covering France from 1958 to 2019 (Quintana-Seguí et al., 2008; Vidal et al., 2010). In addition, 296 wells from the ADES database (Winckel et al., 2022) were used for aquifer system calibration and validation (Fig. 2; in red).

3.2. Numerical hydrological model

The physically-based and distributed CaWaQS[1] model (CAtchment WAter Quality Simulator – Flipo et al., 2007, 2021b, 2023) mimics physical processes controlling water fluxes in large river basins connected to aquifer systems. Partly inherited from de Marsily et al. (1978) and Ledoux et al. (1984, 1989), CaWaQS is a coupled hydrological-hydrogeological model that simulates the main surface and subsurface processes involved in the water cycle at the regional scale, including anthropogenic forcings such as groundwater withdrawals. To transform rainfall into river discharges and hydraulic head in aquifer units at a daily time step, the model first solves the hydrological budget with a conceptual reservoir-based approach (Girard et al., 1980). The infiltrated water is transferred through the vadose zone with a reservoir cascade to reach the surface of the aquifer system (Besbes and De Marsily, 1984). Aquifer modeling concepts include a GW module, based on the pseudo-3-D diffusivity equation resolution (de Marsily, 1986). It accounts for exchanges between aquifer units using a 1-D vertical simplification of fluxes, assumed to be linearly connected to the hydraulic head difference between units. A non-linear conductance procedure, accounting for a limitation of the infiltration flux in case of river-aquifer disconnection (Brunner et al., 2009; Rivière et al., 2014; Newcomer et al., 2016) is implemented within an iterative Picard approach to compute stream–aquifer exchanges (Rushton, 2007; Ebel et al., 2009; Flipo et al., 2014). Finally, discharge routing in the river system is based on a simple Muskingum model (David et al., 2011) coupled with a Manning-Strickler equilibrium at each time step (Saleh et al., 2011). The approach adopted by the model represents a good

[1] CaWaQS is opensource, available under the Eclipse Public Licence v2.0 at https://gitlab.com/cawaqs/cawaqs.

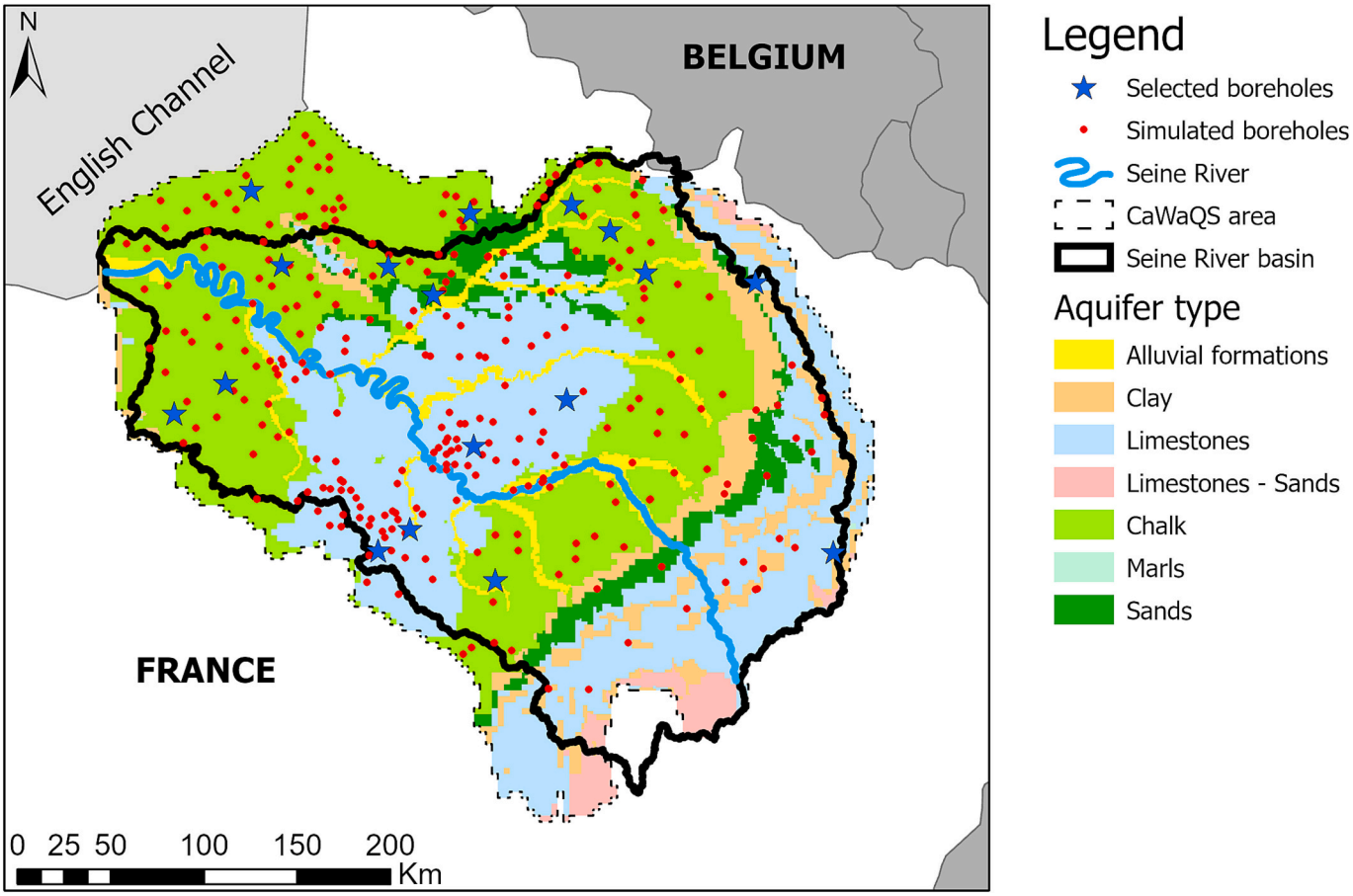

Fig. 2. Study area with all the wells simulated by the CaWaQS model (red points) and the selected wells (blue stars) for the analysis of the sensitivity of GWL to changes in low-frequency climate variability.

compromise between the parsimony of conceptual models such as GR (Perrin et al., 2003) and hyper-resolution models (Wood et al., 2011), from which tools such as Parflow-CLM (O'Neill et al., 2021) are derived. This specific characteristic allows for running multiple simulations at a relatively low computational cost. In addition to the quality of the hydrological processes simulated by the model, an innovative fitting methodology was recently developed to ensure that the model accurately reproduces unmeasured key features of a hydrosystem, such as the partitioning of rainfall into runoff and infiltration, as well as aquifer recharge (Flipo et al., 2023). This work is based on a frequency-domain analysis of river discharge and GWLs in aquifers (Schuite et al., 2019). To the authors' knowledge, CaWaQS is the only Integrated Water Management Model that has been calibrated in both the time and frequency domains. This is particularly important for the present study, as it confirms that the model behaves as a low-pass filter at low frequencies, as expected for a hydrosystem model.

The CaWaQS-Seine basin application (Flipo et al., 2023) is distinctive in its comprehensive representation of the aquifer system, incorporating 20 lithological units beneath the river basin. These units are meshed using multi-scale nested grids with square-shaped cells ranging from 3200 to 100 m in size. From the oldest to the most recent, system units include: (i) an ensemble of aquifer and aquitard units, mostly made of limestone and marl–clay alternation. These units range from the Lower Jurassic (Hettangian stage) to the Lower Cretaceous (Albian stage) and mostly outcrop on the eastern end of the basin, (ii) a large Upper Cretaceous chalk layer, (iii) a 5-layer Tertiary complex ensemble, in the center of the basin, which covers units made of limestone and sand, dating back from the Paleocene to Miocene stages, and (iv) recent alluvial deposits (Pleistocene and Holocene stages) surrounding the main rivers. The remaining crystalline bedrock areas are not explicitly simulated.

3.3. Signal processing approach for generating perturbed GWL scenarios

For this study, seven GWL time series simulated with the CaWaQS software were generated: one reference time series and six perturbed time series. First, a reference scenario for GWL was simulated using the observed precipitation field. Then, perturbed scenarios of GWL were simulated using modified precipitation fields (Fig. 3a). This process is divided into three steps. The first step consisted of identifying significant time scales of low-frequency variability in precipitation (Fig. 3a; Step 1). As reported in previous studies (Massei et al., 2010, 2017; Baulon et al., 2022a, 2022b), significant interannual (2–4 years and 5–8 years) and decadal (~15 years) variability is found in hydroclimate variables (precipitation, streamflow, GWL) of the Seine River Basin. Boé (2020) showed that using the most appropriate downscaled climate model outputs, low frequency variability on the Seine watershed would be over- or underestimated by up to 30 %. Here, these specific timescales of variability in the precipitation field were modified by either increasing or decreasing their amplitude by 50 % (Fig. 3a; Step 2), leading to six scenarios of low-frequency variability in precipitation. Each perturbed precipitation field was finally injected in the CaWaQS software to simulate perturbed GWL (Fig. 3a; Step 3). The sensitivity to changes in precipitation variability only was assessed, the observed temperature field being kept unchanged.

Modification of the spectral content of precipitation was done using wavelet multiresolution analysis. Details about the mathematical basis of wavelet MRA can be found in Percival and Walden (2000), for

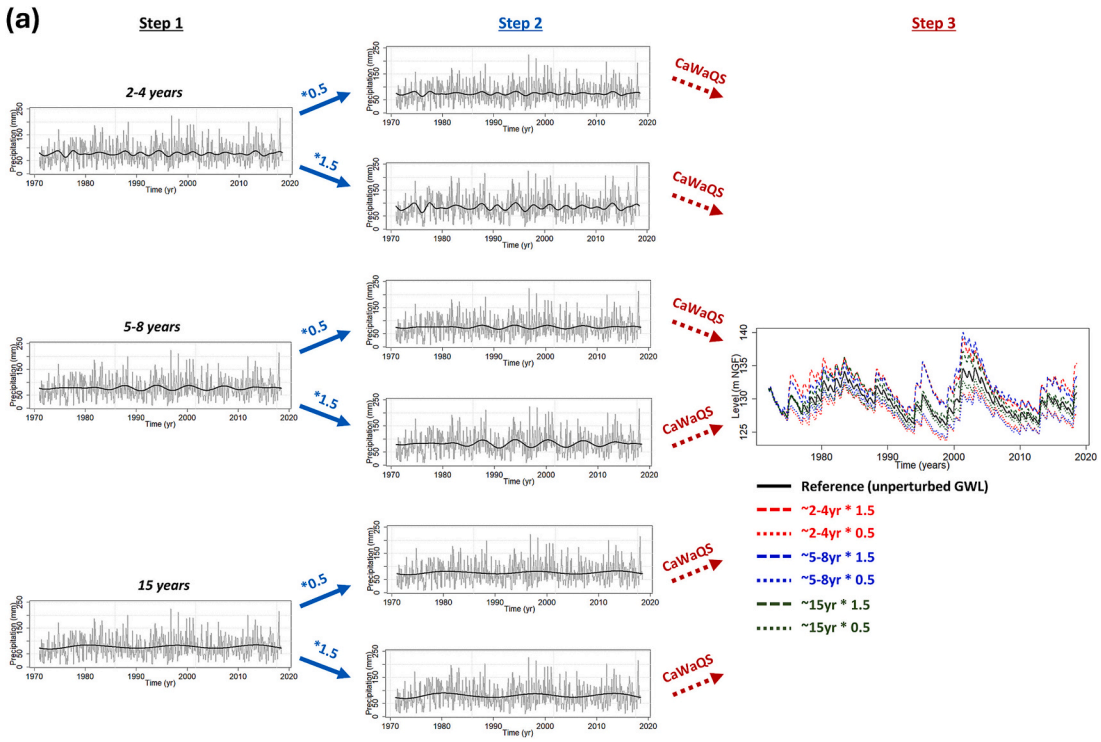

(b)Changes in extreme levels occurrence

Step 1 - Determine the number of high level peaks in the reference and perturbed GWL above percentile 0.8

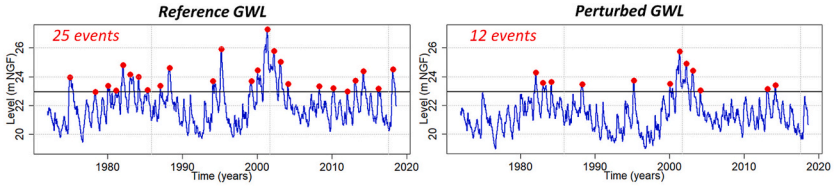

Step 2 - Ratio between the number of events in the perturbed GWL compared to the reference GWL

$$Ratio = \frac{Number\ of\ peaks\ in\ the\ perturbed\ GWL}{Number\ of\ peaks\ in\ the\ reference\ GWL}$$

(c)Changes of the severity of some well-known historical events (e.g. 2001)

Step 1 – Determine the difference between the 2001 high level peak in the reference and perturbed GWL

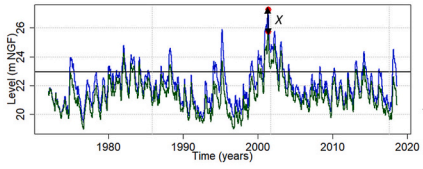

Reference GWL — 2001 HL
Perturbed GWL

$$X = Level\ in\ perturbed\ GWL\ -\ Level\ in\ reference\ GWL$$

Step 2 – Normalize by the maximum water level fluctuation (mWLF) of the reference GWL

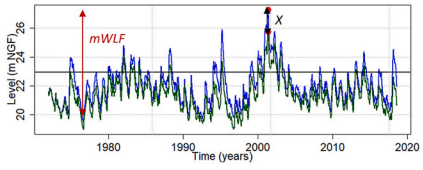

Reference GWL — 2001 HL
Perturbed GWL

$$Importance\ of\ change = \frac{X}{mWLF} * 100$$

Fig. 3. (a) Workflow of perturbed GWL simulation with one well as an example. Step 1 plots indicate in grey the unperturbed precipitation time series and superimposed in black the low-frequency variability. Step 2 plots show in grey the perturbed precipitation time series and in black the low-frequency variability increased or decreased by 50 %. Step 3 plot indicates in color the perturbed GWL and in black, the reference GWL simulated with CaWaQS software. Please note that in this figure, the modification made on precipitation is shown at a monthly time step to better capture and display the low-frequency variability on plots, but the analysis was done at a daily time step in this study. (b-c) Workflow of the sensitivity analysis approach for high and low GWL. Only high levels (HL) above the 80th quantile are presented here for illustrative purposes.

instance. Precipitation time series of the SAFRAN grid were first decomposed into several wavelet components. Then, the amplitude of components corresponding to the desired timescales (namely 2–4 years, 5–8 years and ~15 years) were simply scaled by 0.5 and 1.5, before summing up all components to obtain a modified precipitation time series. This process was applied to each cell of the SAFRAN grid. Details about the wavelet decomposition methodology can be found in many previous studies (e.g. Massei et al., 2017; Baulon et al., 2022a) and are not presented here.

However, for some time periods, the modification of the spectral content can lead to negative precipitation values. These negative values are then replaced by zero values. However, this setting can have important consequences as it creates artificial oscillations (following the repetition of zeros at several points of the time series), which skew the signal input to CaWaQS, and thus the simulation. It is therefore necessary to limit the use of the reset to zero by reducing the mathematical artifacts. We chose to use a multiresolution decomposition method with modified filters introduced by Starck et al. (2007) to ensure that a minimum of negative values is produced by the decomposition, limiting the use of the reset to zero. The Python package "cosmostat" was used for this purpose (Starck et al., 2020).

3.4. Protocol for analyzing the impacts of changes in interannual and decadal precipitation variability on groundwater levels

The analysis of the sensitivity of GWL to changes in interannual to decadal precipitation variability was achieved using 17 wells in the Seine River basin (Fig. 2; blue stars) corresponding to best-simulated GWL time series. These wells were not necessarily located in the same hydrogeologic formation (Seno-Turonian chalk of Normandy in the downstream part of the basin, Eocene to Miocene calcareous aquifers in the center, Seno-Turonian chalk and Jurassic limestones upstream). Only the 1972–2018 period of the GWL time series was considered for the analysis because of a bad simulation of reference GWL on the 1970–1971 period likely due to the warm-up period of the model.

We determined the changes in descriptive statistics (mean, variance, upper and lower quantiles) of the time series by comparing perturbed GWL (each scenario) with the reference GWL. First, we quantified the changes in the average of GWL. To quantify such changes, we calculated the difference between the mean of perturbed GWL and reference GWL for each well. Second, we determined whether changes in the amplitude of interannual and decadal precipitation variability also induce changes in GWL variance in the statistical sense (i.e. mean of squared deviation from the mean). We therefore calculated the ratio between the variance of perturbed GWL and reference GWL.

For the analysis of extreme GWL, we compared the number of extreme high- and low-levels as well as the severity of some well-known historical events of groundwater drought and flooding between perturbed GWL and reference GWL (Fig. 3b–c). These historical events were the 1995 and 2001 high levels, and the 1992 and 1998 low levels, among the most severe groundwater drought and flood events across the Paris Basin during the past decades (Machard de Gramont and Mardhel, 2006; Seguin et al., 2019). Here, we call "extreme levels" the high-level (HL) and low-level (LL) peaks that are above or below quantiles 0.8 and 0.2, respectively. These quantiles were selected to ensure a high enough number of peaks above/below the threshold for the most inertial water tables. For the analysis of both the reference and perturbed GWL, the threshold remains constant and is always set to the quantiles 0.8 and 0.2 of the reference GWL.

To determine changes in the occurrence of extreme levels, we calculated the ratio between the number of peaks (above or below the threshold) in the perturbed GWL and reference GWL (Fig. 3b). Then, to determine to what extent a change of low-frequency variability in precipitation could affect the GWL extreme severity (i.e., magnitude) of some well-known historical events, we calculated the difference between the maximum level during the event in perturbed GWL and the reference GWL (Fig. 3c; Step 1). We then normalized the difference of levels by the maximum water level fluctuation (mWLF) of the reference to assess the importance of the change in the water table maximum variation (Fig. 3c; Step 2).

4. Results

4.1. Impact on average GWLs

Fig. 4 shows to what extent the perturbation of interannual (2–4 years or 5–8 years) and decadal (15 years) variability in precipitation modified the GWL averages. Regardless of the timescale considered, the mean GWL systematically decreases when low-frequency precipitation variability is damped by 50 % (*0.5 scenarios; Fig. 4a). Conversely, the average GWL increases when the amplitude of interannual and decadal variations is enhanced by 50 % (*1.5 scenarios; Fig. 4a). Notice that similar results can be observed for winter precipitation (Supplementary material 1). However, the magnitude of the increase or decrease depends on the aquifer properties and the variability perturbed in precipitation (Fig. 4a–b). Inertial water tables (Fig. 4b, i. and ii.) exhibit the greatest increases or decreases of the mean GWL in response to changes in precipitation variability. In contrast, the most reactive water tables exhibit the lowest increases and decreases (Fig. 4b, iii. and iv.). The GWL average seems to be slightly more sensitive to the perturbation of the 2–4 years variability than the 5–8 years variability, and conversely less sensitive to the perturbation of the 15 years variability (Fig. 4a). In addition, GWLs often increase more when low-frequency precipitation variability is enhanced (*1.5) than they decrease when precipitation variability is dampened (*0.5). We also note that perturbed GWLs increase (*1.5) or decrease (*0.5) more during high-level periods than low-level periods, and this is even more striking for inertial water tables (Fig. 4b).

4.2. Impact on GWL variance

The perturbation of precipitation variability is directly reflected in GWLs (Fig. 5). The modifications of GWL variance follow the same increasing (*1.5 scenarios) or decreasing (*0.5 scenarios) trends as for the GWL average. Similar results can be observed for winter precipitation (Supplementary material 2). However, while the variance modification is spatially homogeneous in precipitation, it is much less homogeneous for GWL as it depends on the aquifer properties. Therefore, GWL variance modification is also not the same according to the perturbed precipitation variability (Fig. 5). For instance, the greatest increase of variance in the Beauce limestones (western part in the middle of the basin) is observed when the ~15-yr variability is enhanced in precipitation. This is probably because the ~15-yr variability represents the largest part of total GWL variance (Baulon et al., 2022b). Similarly, the biggest increase of variance in the Seno-Turonian chalk of Normandy (downstream part of the basin) is observed when the 5-8 yr precipitation variability is enhanced. In addition, variance modifications either in winter precipitation or GWL are always greater when the low-frequency variability is enhanced than when it is damped.

4.3. Impact on high and low GWL occurrence

In previous sections, we observed that the GWL mean is often significantly affected by changes in low-frequency climate variability. In this section, we analyze to what extent extreme GWL may also be affected.

The perturbation tests often led to a significant modification of HL and LL occurrence in GWL (Fig. 6). Given the increase in mean GWL when low-frequency variability is enhanced by 50 % (*1.5 scenario) in precipitation, this perturbation led to a decreased LL occurrence and an increased HL occurrence in GWL. Conversely, the 50 % decrease in low-frequency precipitation variability led to an increased LL occurrence and

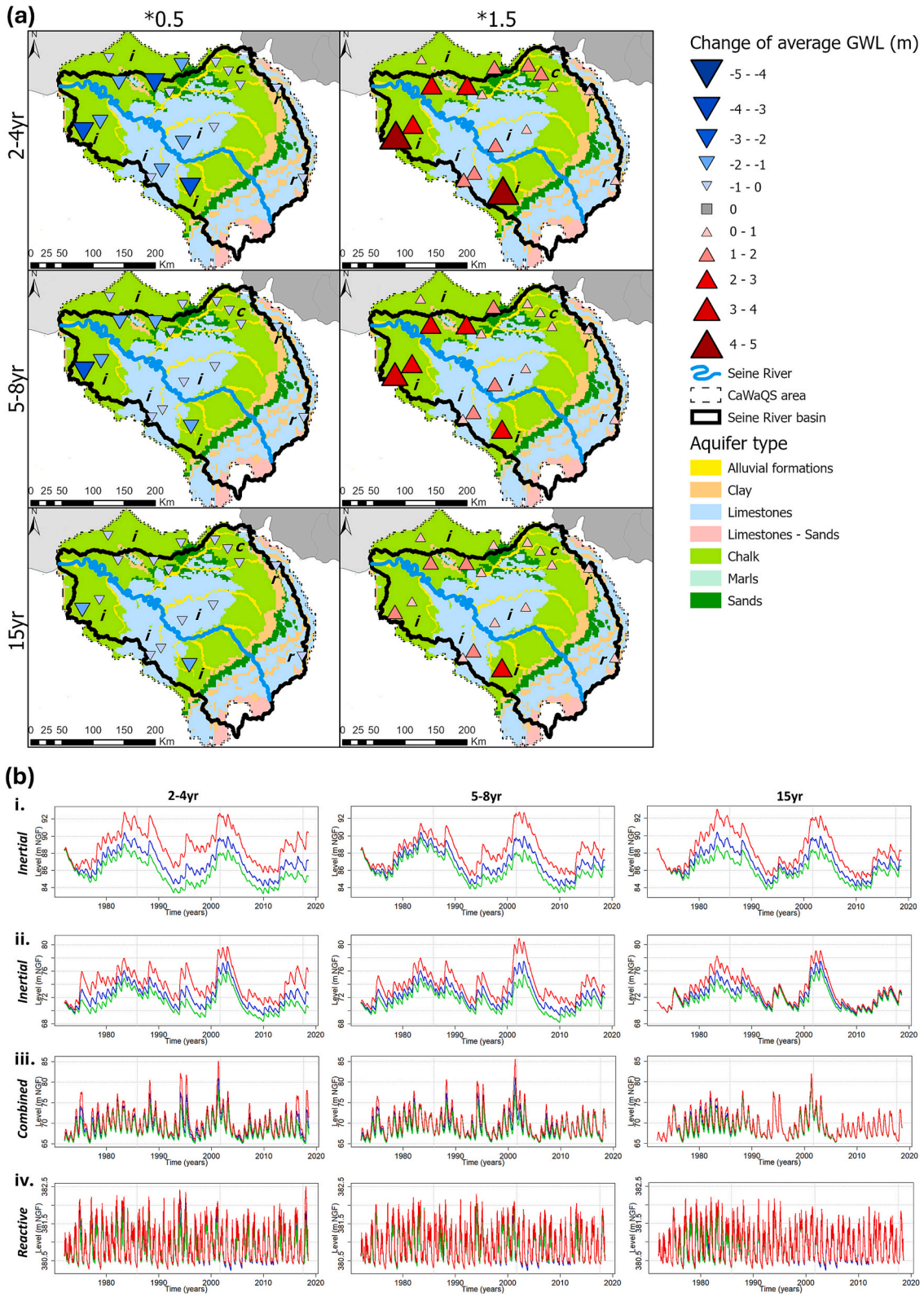

Fig. 4. (a) Change in average of GWLs (m) for each scenario of perturbed low-frequency precipitation variability. Red (blue) triangles indicate an increase (decrease) of GWL mean. The letters on the map indicate the water table dynamic: "i" for inertial, "c" for combined, "r" for reactive. (b) Reference and perturbed GWLs for wells monitoring various aquifer and water table dynamics: i. the Miocene limestones of Beauce in the middle part of the basin with the well of Briarres-Sur-Essonne (inertial); ii. the Seno-Turonian chalk of Picardy in the downstream part of the basin with the well of Liancourt-Fosse (inertial); iii. the Seno-Turonian chalk of Aisne in the upstream part of the basin with the well of Parpeville (combined dynamic); iv. the Jurassic limestones in the upstream part of the basin with the well of Cuves (reactive). The reference GWLs are in blue, the *1.5 scenarios are in red, and the *0.5 scenarios are in green.

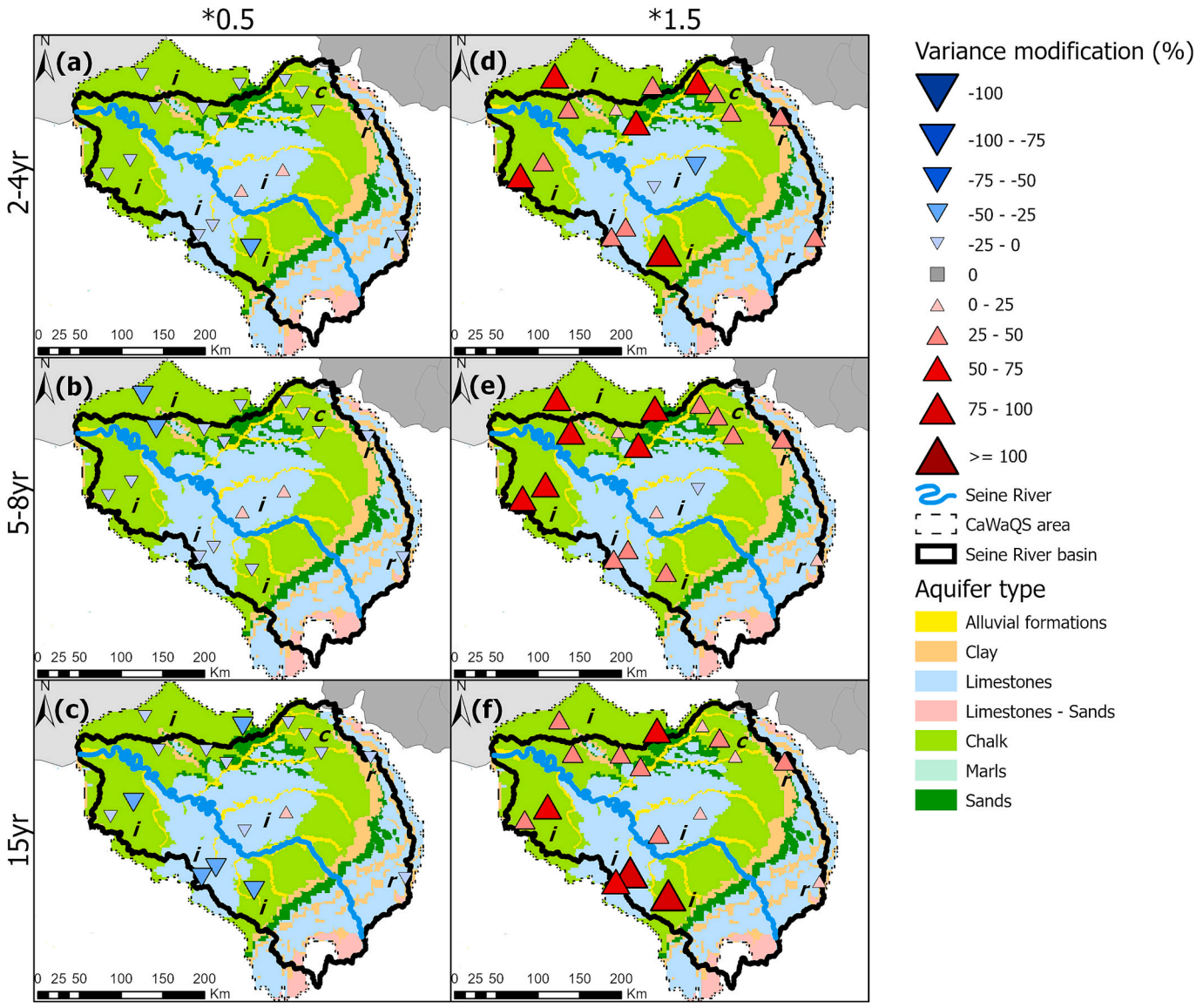

Fig. 5. Variance modification (%) between perturbed GWL and the reference GWL for each scenario. Blue triangles indicate a decreased variance in perturbed GWL compared to the reference. Red triangles indicate an increased variance in perturbed GWL compared to the reference. The letters on the map indicate the water table dynamic: "i" for inertial, "c" for combined, "r" for reactive.

a decreased HL occurrence. HL and LL occurrences in GWL were often significantly affected when 2-4 yr or 5-8 yr timescales of precipitation variability were modified, whereas modification of the 15-yr variability had a much lower impact. The 15-yr variability perturbation affected HL and LL occurrence more in South-West limestones (Beauce) compared to other aquifers. Finally, changes in interannual to decadal climate variability affected HL and LL occurrences more in aquifers of inertial types than in aquifers with reactive types.

4.4. Focus on particular events: impact on events severity

The impact of these changes on the severity of events was also evaluated. We focused on four specific events which are the severest high and low GWL events ever recorded in the Paris basin: 1992 and 1998 for low levels, 1995 and 2001 for high levels.

Overall, decreasing (increasing) the amplitude of precipitation low-frequency variability always led to an increased (decreased) severity of LL events and decreased (increased) severity of HL events (Figs. 7–8). In other words, LL (resp. HL) are lower (resp. higher) when low-frequency variability is decreased (resp. increased). However, the magnitude of increase/decrease differs between the 1992 LL and 1998 LL (Fig. 7), and between the 1995 HL and 2001 HL (Fig. 8). The modification of the event severity seems to be greater for the 1998 LL than the 1992 LL over the Seine River basin (Fig. 7). In addition, this modification depends on the borehole considered: for the same event, the levels of some wells were only slightly modified while those of others were strongly modified (Figs. 7–8). As in previous sections, extreme GWL were more sensitive to the perturbation of 2-4 yr and 5-8 yr variabilities than the perturbation of 15 yr variability.

Furthermore, the influence of the low-frequency perturbation in precipitation appeared to be stronger on HL than LL (Figs. 7–8). This may at least partly be explained by the substitution of negative values in daily precipitation by zero which prevents low precipitation amounts from decreasing to very low values, and dampens the influence of the perturbation for the low amounts. Conversely, high precipitation values after perturbation can rise to a very high level without limitation. And this phenomenon may also affect extreme GWL in the same way. The other interesting result is that the 2001 HL event seems to be more affected by the perturbation of the ~15-yr variability than the 1995 HL event (Fig. 8). This might be linked to the large contribution of the ~15-

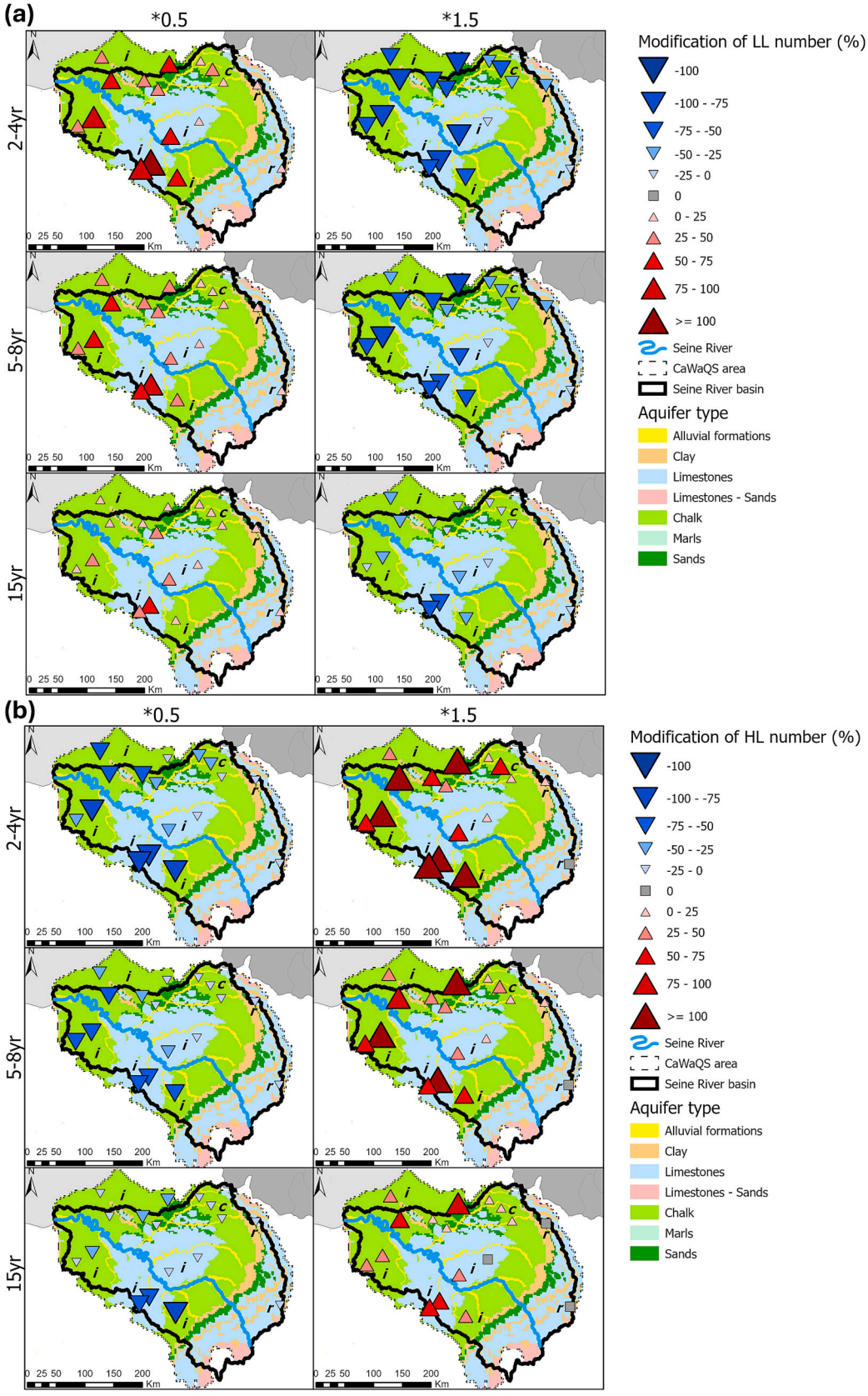

Fig. 6. (a) Modification of groundwater low level (LL) number (%) for each scenario of perturbed low-frequency variability in precipitation. The letters indicate the water table dynamic: "i" for inertial, "c" for combined, "r" for reactive. (b) Same but for groundwater high level (HL).

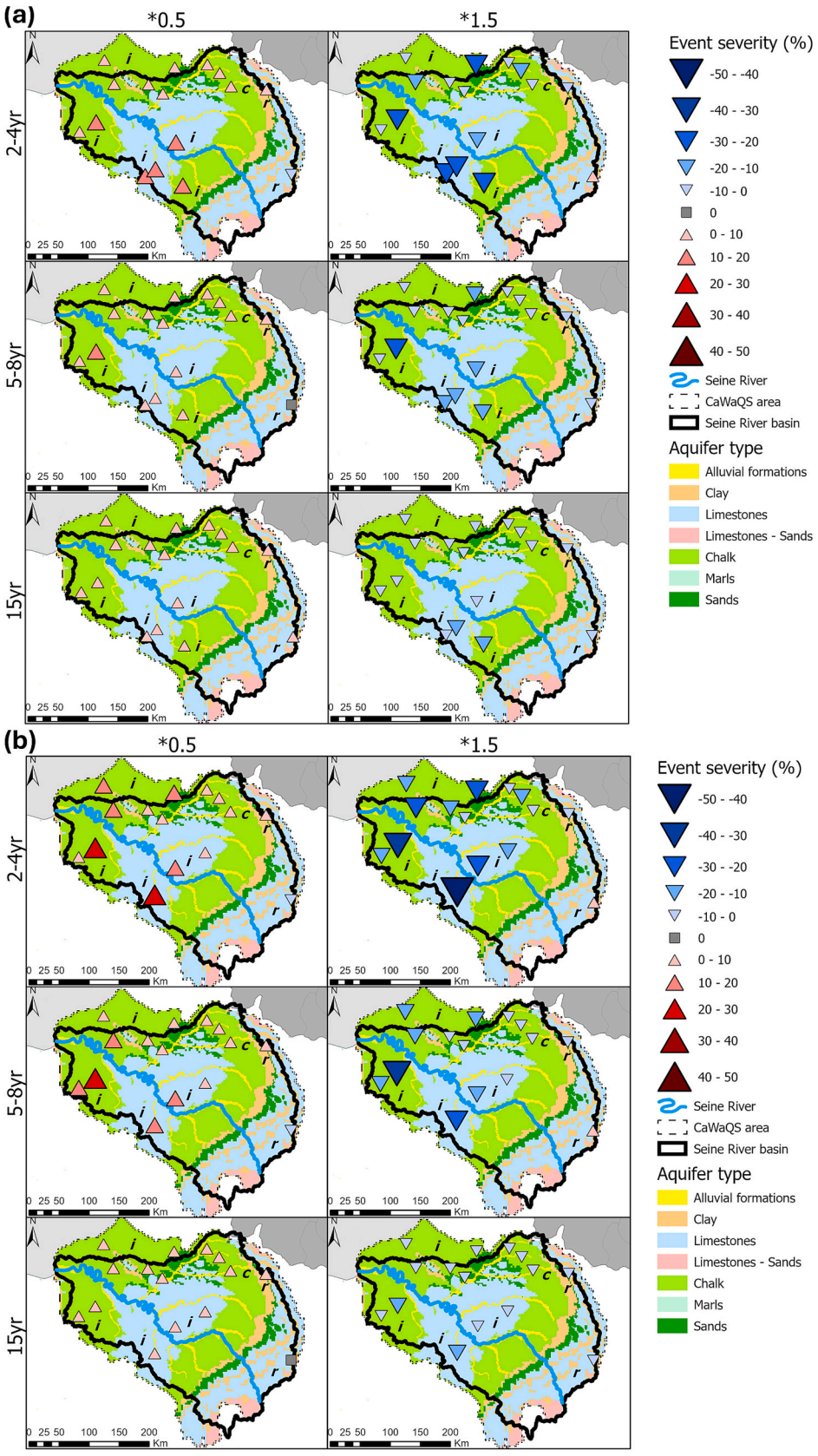

Fig. 7. (a) Increase/decrease of the 1992 LL event severity (% of the maximum water level fluctuation) for each scenario of perturbed low-frequency variability in precipitation. Here, the severity expresses the difference in level during the 1992 event between perturbed GWL and reference GWL normalized by the maximum water level fluctuation. Blue triangles represent a decreased severity of the event in perturbed GWL (i.e. higher groundwater levels), while red triangles represent an increased severity (i.e. lower groundwater levels). A missing well indicates that the 1992 event was not identified as an extreme level for this well. The letters on the map indicate the water table dynamic: "i" for inertial, "c" for combined, "r" for reactive. (b) Same for the 1998 groundwater LL event.

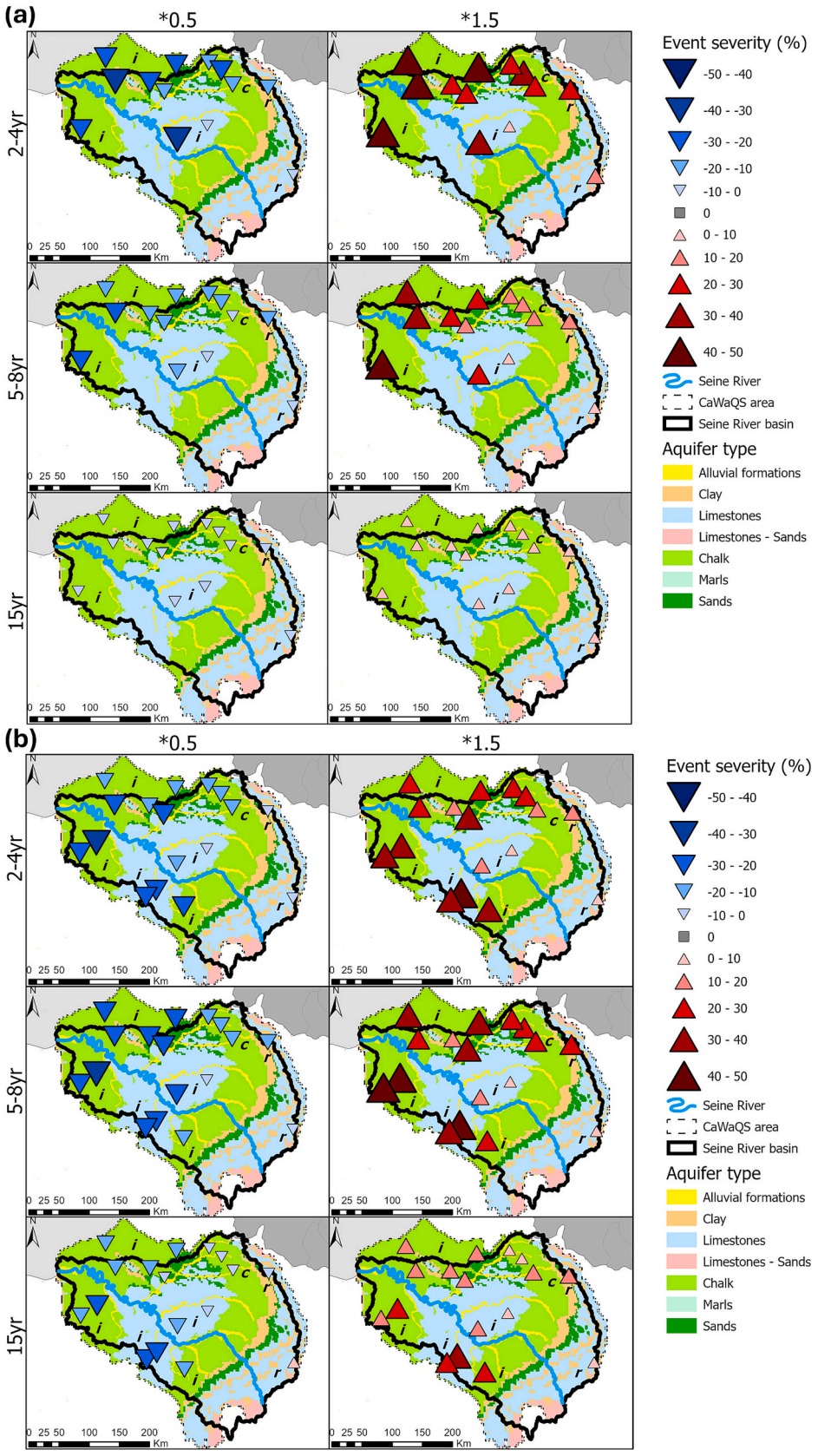

Fig. 8. (a) Increase/decrease of the 1995 HL event severity (% of the maximum water level fluctuation) for each scenario of perturbed low-frequency variability in precipitation. Here, the severity expresses the difference in level during the 1995 event between perturbed GWL and reference GWL normalized by the maximum water level fluctuation. Blue triangles represent a decreased severity of the event in perturbed GWL (i.e., lower groundwater levels), while red triangles represent an increased severity (i.e., higher groundwater levels). A missing well indicates that the 1995 event was not identified as an extreme level for that well. The letters on the map indicate the water table dynamic: "i" for inertial, "c" for combined, "r" for reactive. (b) Same for the 2001 groundwater HL event.

yr variability to the emergence of the 2001 HL event over the Seine River basin (Baulon et al., 2022b).

5. Discussion and conclusion

This study aimed at investigating to what extent GWL are sensitive to the low-frequency variability (interannual to decadal) of precipitation that originates from large-scale climate variability. In particular, three different types of GWL variability may exist (inertial, reactive, mixed-type), that likely exhibit different sensitivities to low-frequency variability. Numerical experiments were then conducted to simulate the effect of different amplitudes of climate low-frequency variability on GWL. For the sake of simplicity, only precipitation was considered herein: the low-frequency variability amplitude of precipitation was modified using signal processing methods, resulting in altered precipitation fields that were used as input to a numerical hydrological model previously calibrated on the study area (Seine River basin).

The motivation behind this study was dictated by previous knowledge about the impact of low-frequency variability on hydrological variability. Numerous studies have pointed out the existence and importance of the underlying low-frequency behavior of precipitation, temperature, evapotranspiration, streamflow, runoff, and GWLs (Massei et al., 2010; Gudmundsson et al., 2011; Holman et al., 2011; Dieppois et al., 2013, 2016; Matti et al., 2017; Liesch and Wunsch, 2019; Fossa et al., 2021; Baulon et al., 2022b). Albeit of very small amplitude in precipitation, the low-pass filtering effect of watersheds and aquifers tends to enhance the expression of low-frequency variability in hydrological responses. As emphasized in these studies, low-frequency variability is mainly linked to the stochastic nature of internal climate variability. Low-frequency variability has long been proven to significantly affect the occurrence and intensity of hydrological trends and extreme levels (Hannaford et al., 2013; Peña-Angulo et al., 2020; Baulon et al., 2022a, 2022b). For instance, Baulon et al. (2022a) showed that GWL trends may be affected by the amplitude of low-frequency variability in the GWL signal. More generally, several studies highlighted how internal climate low-frequency variability could amplify or hide the effects of climate change on meteorological and hydrological variables (Fatichi et al., 2014; Martel et al., 2018; Gu et al., 2019). However, either naturally or as a result of anthropogenic climate change, the amplitude of low-frequency variability originating from internal modes of climate variability may increase or decrease (Lenton et al., 2008; Dong et al., 2011; Caesar et al., 2018; He and Li, 2019), which could significantly affect the major hydrological trends; hence the need to address this issue.

Furthermore, some studies have shown that climate models do not correctly reproduce low-frequency climate variability (Qasmi et al., 2017; Boé, 2020; Eade et al., 2022), because internal climate variability is purely stochastic. It is therefore difficult to reproduce any one of many possible outcomes. As a result, 75 % of the CMIP6 models overestimate interannual variability in winter and spring over the Seine River basin. In summer and autumn, around half and two-thirds of the models are respectively consistent with observations (Boé, 2020). Such results have implications for climate projections (and then hydrological projections), as internal low-frequency climate variability is difficult to predict. Low-frequency climate variability therefore introduces considerable uncertainty into climate projections, which can be as large as the uncertainties introduced by the climate model (Terray and Boé, 2013). Moreover, some scenarios of changes in low-frequency climate variability may not be covered by climate projections. It is therefore necessary to create them artificially to get the desired changes in low-frequency climate variability and to explore the impact on groundwater resources, which is what is done in this study.

Our study showed that any change in interannual to decadal climate variability would lead to substantial changes in GWL mean, variance, and extremes. The present study underlines the complex response of GWL to changes in climate low-frequency variability, as we observed: i) not only a modification of GWL variance but also a modification of GWL mean (increase or decrease according to the scenario), ii) the GWL response to precipitation perturbation is not linear, varying according to the aquifer, but all aquifers are affected. In general, overestimating low-frequency variability in precipitation by 50 % led to overestimated GWL, overestimated groundwater flood occurrence and severity, and underestimation of the occurrence and severity of groundwater droughts. Conversely, underestimating low-frequency variability in precipitation by 50 % may lead to underestimated GWL, overestimation of the occurrence and severity of groundwater droughts, and underestimated groundwater flood occurrence and severity.

All aquifers in the Seine River basin are affected by changes in low-frequency climate variability, although not all to the same magnitude, depending on the aquifer. This, of course, depends on their physical characteristics and their capacity to modulate/accentuate/mitigate such low-frequency components. The physical parameters known to control the GWL dynamic and the significance of low-frequency variability within the groundwater signal are: the thickness and lithology of surficial formations, aquifer thickness and lithology, vadose zone thickness, hydraulic diffusivity, upstream/downstream location along the flow path, distance to the river, and presence of karst (Slimani et al., 2009; El Janyani et al., 2012, 2014; Schuite et al., 2019; Liesch and Wunsch, 2019; Haaf et al., 2020).

Reactive water tables are least affected by changes in low-frequency climate variability. The increase (decrease) in GWLs remains moderate (up to $\pm/-1$ m at most) when low-frequency climate variability increases (decreases). The severity of the groundwater low levels of 1992 and 1998 is increased by 10 % if the low-frequency climate variability decreases, and the severity of the groundwater high levels of 1995 and 2001 is increased by 30 % (maximum value) if the low-frequency climate variability increases. These results are closely related to the physical characteristics of this type of aquifer, which in the case of Jurassic limestone is particularly old and highly fractured, explaining the reactive dynamic of the water table, with dominant annual variations (Roux, 2006; Baulon et al., 2022a). As extreme GWLs for this groundwater dynamic are highly dependent on the annual variability and therefore on the winter recharge in the current hydrological year, these changes do not imply any major changes in groundwater management. However, the average change in levels should be considered, as it may lead to more severe extremes (droughts in the case of decreasing low-frequency climate variability and high levels in the case of increasing) but remains moderate compared to other types of aquifers. These aquifers remain relatively unaffected by changes in low-frequency climate variability.

Conversely, inertial water tables are significantly affected by these changes in low-frequency climate variability. GWLs may rise (due to increased low-frequency climate variability) or fall (decreased low-frequency climate variability) significantly by up to $+5$ m and -3 m, respectively. Extreme GWLs are consequently more frequent and more severe, entailing more droughts with increasing severity if low-frequency climate variability decreases, and more high levels, also with increasing severity if low-frequency climate variability increases. For inertial water tables, this can result in up to 100 % more high/low levels than observed, with extreme events increasing in severity (amplitude) by 50 %. The variance of GWLs can also increase by 75 to 100 % when low-frequency climate variability is amplified. This phenomenon is less pronounced (up to -50 %) when low-frequency climate variability is reduced. These results are also closely related to the physical characteristics of this type of aquifer, which in the case of Tertiary limestone and Cretaceous chalk (although also fractured) constitute large reservoirs with a considerable unsaturated zone and often considerable thickness of the surficial formations and low hydraulic diffusivity (except in karst areas), which explains the considerable inertia of these aquifers, with dominant interannual and decadal variations (Slimani et al., 2009; El Janyani et al., 2012; Baulon et al., 2022b). As such geological formations exhibit water tables whose

fluctuations are largely dependent on low-frequency climate variability; the study shows that they are highly sensitive to changes in low-frequency climate variability. Consequently, these changes may affect groundwater management, particularly the management of extreme GWLs (groundwater floods and droughts).

Finally, mixed water tables are often affected quite significantly by changes in low-frequency climate variability, but often less so than inertial water tables. GWLs may rise (due to increased low-frequency climate variability) or fall (decreased low-frequency climate variability) by up to +2 m and −1 m, respectively. As a result, a 75 % increase in the number of high levels compared to what is observed is identified when low-frequency variability increases, with the severity of the high levels in 1995 and 2001 also increasing by 40 %. Low levels are generally less affected as low-frequency climate variability decreases, with a 50 % increase in the number of low levels compared to what was observed, and only a 10 % increase in the severity of the 1992 and 1998 droughts.

We can conclude from this study that any change in low-frequency climate variability has therefore a significant impact on GWLs, and the use of biased precipitation data due to an under- or overestimated low-frequency variability may lead to significant discrepancies in GWLs. This result is particularly relevant for aquifers with inertial or mixed behaviors of water tables, in which water stocks and levels are primarily controlled by interannual and decadal climate variability.

The advantage of the study area analyzed (Seine River basin) is that it includes a wide variety of GWL behaviors (reactive, mixed, inertial) that restitute low-frequency variability to a small or large extent. It thus allows us to analyze the changes that changes in low-frequency climate variability can induce on GWLs in systems that include a wide variety of GWL responses. Therefore, a similar analysis in other geological contexts (granitic, volcanic, alluvial) would not, in principle, provide additional information on the GWL response to changes in low-frequency climate variability.

This study underlines potentially major consequences regarding (i) the potential changes in low-frequency climate variability under climate change on GWLs, (ii) long-term GWL projection as developed in many previous studies (Azizi et al., 2021; Wunsch et al., 2022; Vergnes et al., 2023). Since interannual to decadal variations from internal modes of climate variability (e.g., NAO, ENSO) are not easily predictable, precipitation projections may be subject to strong uncertainties regarding low-frequency variability (e.g. Terray and Boé, 2013; Boé, 2020). Then, the corresponding uncertainties propagate through hydrogeological models, resulting in a strong uncertainty of GWL projections.

However, for future work some improvements could be made to better answer the question, particularly on the input variables. First, internal modes of climate variability affect not only precipitation, but also temperature (Fossa et al., 2021; Dieppois et al., 2013). Consequently, changes in large-scale climate variability would necessarily affect temperature low-frequency variability too. The perturbation of interannual to decadal temperature variability would therefore have been valuable for a more accurate analysis since temperature may significantly affect groundwater recharge (McCallum et al., 2010) because it is an important driver of evaporation and evapotranspiration (Oudin et al., 2005; McMahon et al., 2013). It is not clear however, whether interannual to decadal variability in temperature should be perturbed with the same coefficients as those used for precipitation. In other words, if precipitation decadal variability increases by 50 %, this does not mean that temperature decadal variability also increases by 50 %.

In addition, interannual and decadal variability are perturbed one at a time, while each timescale interacts with the others (Fossa et al., 2021). Timescale interactions are at the origin of the highly non-linear behavior between forcing factors and hydrological responses. These interactions occur not only within the climate system itself, but also at the level of the hydrosystem. In their study, Fossa et al. (2021) showed which timescales influence others and the nature of the linkages (phase, amplitude) between timescales. For instance, they highlighted that for the area used in our study, the 5–8 year variability would drive the variability of smaller timescales (2–4 year) in precipitation. Considering such a cross-scale relationship in the present analysis would have required a better overview and understanding of all the processes involved, but it could be an interesting topic to explore for future work on the subject.

Supplementary data to this article can be found online at https://doi.org/10.1016/j.scitotenv.2024.177636.

CRediT authorship contribution statement

Lisa Baulon: Writing – original draft, Visualization, Software, Methodology, Investigation, Formal analysis, Data curation, Conceptualization. **Manuel Fossa:** Writing – review & editing, Visualization, Software, Methodology, Investigation, Formal analysis, Data curation, Conceptualization. **Nicolas Massei:** Writing – review & editing, Validation, Supervision, Project administration, Methodology, Investigation, Funding acquisition, Conceptualization. **Nicolas Flipo:** Writing – review & editing, Visualization, Validation, Supervision, Software, Project administration, Methodology, Investigation, Funding acquisition, Formal analysis, Conceptualization. **Nicolas Gallois:** Writing – review & editing, Visualization, Software, Methodology, Investigation, Formal analysis, Data curation, Conceptualization. **Matthieu Fournier:** Writing – review & editing, Visualization, Validation, Supervision, Methodology, Investigation. **Bastien Dieppois:** Writing – review & editing, Visualization, Validation, Supervision, Methodology, Investigation, Conceptualization. **Luminita Danaila:** Writing – review & editing, Visualization, Validation, Supervision, Methodology, Conceptualization. **Delphine Allier:** Writing – review & editing, Visualization, Validation. **Hélène Bessiere:** Writing – review & editing, Visualization, Validation.

Declaration of competing interest

The authors declare that they have no known competing financial interests or personal relationships that could have appeared to influence the work reported in this paper.

Acknowledgements

We would like to thank the PIREN Seine program, Agence de l'Eau Seine Normandie (AquiVar and AquiVar+ projects), BRGM and the Normandy region for the financial support. We would also like to thank Julien Boé for helpful discussions on the project.

Data availability

Data will be made available on request.

References

Azizi, H., Ebrahimi, H., Mohammad Vali Samani, H., Khaki, V., 2021. Evaluating the effects of climate change on groundwater level in the Varamin plain. Water Supply 21, 1372–1384. https://doi.org/10.2166/ws.2021.007.

Baulon, L., Allier, D., Massei, N., Bessiere, H., Fournier, M., Bault, V., 2022a. Influence of low-frequency variability on groundwater level trends. J. Hydrol. 606, 127436. https://doi.org/10.1016/j.jhydrol.2022.127436.

Baulon, L., Massei, N., Allier, D., Fournier, M., Bessiere, H., 2022b. Influence of low-frequency variability on high and low groundwater levels: example of aquifers in the Paris Basin. Hydrol. Earth Syst. Sci. 26, 2829–2854. https://doi.org/10.5194/hess-26-2829-2022.

Besbes, M., De Marsily, G., 1984. From infiltration to recharge: use of a parametric transfer function. J. Hydrol. 74, 271–293. https://doi.org/10.1016/0022-1694(84)90019-2.

Blöschl, G., Bierkens, M.F.P., Chambel, A., Cudennec, C., Destouni, G., Fiori, A., Kirchner, J.W., McDonnell, J.J., Savenije, H.H.G., Sivapalan, M., Stumpp, C., Toth, E., Volpi, E., Carr, G., Lupton, C., Salinas, J., Széles, B., Viglione, A., Aksoy, H., Allen, S.T., Amin, A., Andréassian, V., Arheimer, B., Aryal, S.K., Baker, V., Bardsley, E., Barendrecht, M.H., Bartosova, A., Batelaan, O., Berghuijs, W.R.,

Beven, K., Blume, T., Bogaard, T., Borges de Amorim, P., Böttcher, M.E., Boulet, G., Breinl, K., Brilly, M., Brocca, L., Buytaert, W., Castellarin, A., Castelletti, A., Chen, X., Chen, Yangbo, Chen, Yuanfang, Chifflard, P., Claps, P., Clark, M.P., Collins, A.L., Croke, B., Dathe, A., David, P.C., de Barros, F.P.J., de Rooij, G., Di Baldassarre, G., Driscoll, J.M., Duethmann, D., Dwivedi, R., Eris, E., Farmer, W.H., Feiccabrino, J., Ferguson, G., Ferrari, E., Ferraris, S., Fersch, B., Finger, D., Foglia, L., Fowler, K., Gartsman, B., Gascoin, S., Gaume, E., Gelfan, A., Geris, J., Gharari, S., Gleeson, T., Glendell, M., Gonzalez Bevacqua, A., González-Dugo, M.P., Grimaldi, S., Gupta, A.B., Guse, B., Han, D., Hannah, D., Harpold, A., Haun, S., Heal, K., Helfricht, K., Herrnegger, M., Hipsey, M., Hlaváčiková, H., Hohmann, C., Holko, L., Hopkinson, C., Hrachowitz, M., Illangasekare, T.H., Inam, A., Innocente, C., Istanbulluoglu, E., Jarihani, B., Kalantari, Z., Kalvans, A., Khanal, S., Khatami, S., Kiesel, J., Kirkby, M., Knoben, W., Kochanek, K., Kohnová, S., Kolechkina, A., Krause, S., Kreamer, D., Kreibich, H., Kunstmann, H., Lange, H., Liberato, M.L.R., Lindquist, E., Link, T., Liu, J., Loucks, D.P., Luce, C., Mahé, G., Makarieva, O., Malard, J., Mashtayeva, S., Maskey, S., Mas-Pla, J., Mavrova-Guirguinova, M., Mazzoleni, M., Mernild, S., Misstear, B.D., Montanari, A., Müller-Thomy, H., Nabizadeh, A., Nardi, F., Neale, C., Nesterova, N., Nurtaev, B., Odongo, V.O., Panda, S., Pande, S., Pang, Z., Papacharalampous, G., Perrin, C., Pfister, L., Pimentel, R., Polo, M.J., Post, D., Prieto Sierra, C., Ramos, M.-H., Renner, M., Reynolds, J.E., Ridolfi, E., Rigon, R., Riva, M., Robertson, D.E., Rosso, R., Roy, T., Sá, J.H.M., Salvadori, G., Sandells, M., Schaefli, B., Schumann, A., Scolobig, A., Seibert, J., Servat, E., Shafiei, M., Sharma, A., Sidibe, M., Sidle, R.C., Skaugen, T., Smith, H., Spiessl, S.M., Stein, L., Steinsland, I., Strasser, U., Su, B., Szolgay, J., Tarboton, D., Tauro, F., Thirel, G., Tian, F., Tong, R., Tussupova, K., Tyralis, H., Uijlenhoet, R., van Beek, R., van der Ent, R.J., van der Ploeg, M., Van Loon, A.F., van Meerveld, I., van Nooijen, R., van Oel, P.R., Vidal, J.-P., von Freyberg, J., Vorogushyn, S., Wachniew, P., Wade, A.J., Ward, P., Westerberg, I.K., White, C., Wood, E.F., Woods, R., Xu, Z., Yilmaz, K.K., Zhang, Y., 2019. Twenty-three unsolved problems in hydrology (UPH) – a community perspective. Hydrol. Sci. J. 64, 1141–1158. https://doi.org/10.1080/02626667.2019.1620507.

Boé, J., 2020. Résultats des nouvelles projections climatiques sur le bassin de la Seine et évaluation de leur capacité à simuler la variabilité basse-fréquence. Rapport annuel de la phase VIII du PIREN-Seine (16 pp.). https://www.piren-seine.fr/sites/default/files/piren_documents/rapports_dactivite_2020/a1b2_boe_piren_2020_vf.pdf.

Boé, J., Habets, F., 2014. Multi-decadal river flow variations in France. Hydrol. Earth Syst. Sci. 18, 691–708. https://doi.org/10.5194/hess-18-691-2014.

Bonnet, R., Boé, J., Habets, F., 2020. Influence of multidecadal variability on high and low flows: the case of the Seine basin. Hydrol. Earth Syst. Sci. 24, 1611–1631. https://doi.org/10.5194/hess-24-1611-2020.

Brunner, P., Cook, P.G., Simmons, C.T., 2009. Hydrogeologic controls on disconnection between surface water and groundwater. Water Resour. Res. 45. https://doi.org/10.1029/2008WR006953.

Caesar, L., Rahmstorf, S., Robinson, A., Feulner, G., Saba, V., 2018. Observed fingerprint of a weakening Atlantic Ocean overturning circulation. Nature 556, 191–196. https://doi.org/10.1038/s41586-018-0006-5.

Chávez García Silva, R., Reinecke, R., Copty, N.K., Barry, D.A., Heggy, E., Labat, D., Roggero, P.P., Borchardt, D., Rode, M., Gómez-Hernández, J.J., Jomaa, S., 2024. Multi-decadal groundwater observations reveal surprisingly stable levels in southwestern Europe. Commun. Earth Environ. 5, 1–10. https://doi.org/10.1038/s43247-024-01554-w.

Chidepudi, S.K.R., Massei, N., Jardani, A., Henriot, A., Allier, D., Baulon, L., 2023. A wavelet-assisted deep learning approach for simulating groundwater levels affected by low-frequency variability. Sci. Total Environ. 865, 161035. https://doi.org/10.1016/j.scitotenv.2022.161035.

Chidepudi, S.K.R., Massei, N., Jardani, A., Henriot, A., 2024a. Groundwater level reconstruction using long-term climate reanalysis data and deep neural networks. J. Hydrol. Reg. Stud. 51, 101632. https://doi.org/10.1016/j.ejrh.2023.101632.

Chidepudi, S.K.R., Massei, N., Jardani, A., Henriot, A., Fournier, M., Dieppois, B., 2024b. Groundwater level projections for aquifers affected by annual to decadal hydroclimate variations. Earth's. Future. https://doi.org/10.22541/essoar.172526712.23981307/v1 submitted.

David, C., Habets, F., Maidment, D., Yang, Z.-L., 2011. RAPID applied to the SIM-France model. Hydrol. Process. 25, 3412–3425. https://doi.org/10.1002/hyp.8070.

de Marsily, G., 1986. Quantitative hydrogeology. Academic Press, Inc., Orlando, FL.

de Marsily, G., Ledoux, E., Levassor, A., Poitrinal, D., Salem, A., 1978. Modelling of large multilayered aquifer systems: theory and applications. J. Hydrol. 36, 1–33. https://doi.org/10.1016/0022-1694(78)90034-3.

Dieppois, B., Durand, A., Fournier, M., Massei, N., 2013. Links between multidecadal and interdecadal climatic oscillations in the North Atlantic and regional climate variability of northern France and England since the 17th century. J. Geophys. Res.: Atmos. 118, 4359–4372. https://doi.org/10.1002/jgrd.50392.

Dieppois, B., Lawler, D., Slonosky, V., Massei, N., Bigot, S., Fournier, M., Durand, A., 2016. Multidecadal climate variability over northern France during the past 500 years and its relation to large-scale atmospheric circulation. Int. J. Climatol. 36 (15), 4679–4696. https://doi.org/10.1002/joc.4660.

Dong, B., Sutton, R.T., Woollings, T., 2011. Changes of interannual NAO variability in response to greenhouse gases forcing. Climate Dynam. 37, 1621–1641. https://doi.org/10.1007/s00382-010-0936-6.

Douville, H., Raghavan, K., Renwick, J., Allan, R.P., Arias, P.A., Barlow, M., Cerezo-Mota, R., Cherchi, A., Gan, T.Y., Gergis, J., Jiang, D., Khan, A., Pokam Mba, W., Rosenfeld, D., Tierney, J., Zolina, O., 2021. Water cycle changes. In: Masson-Delmotte, V., Zhai, P., Pirani, A., Connors, S.L., Péan, C., Berger, S., Caud, N., Chen, Y., Goldfarb, L., Gomis, M.I., Huang, M., Leitzell, K., Lonnoy, E., Matthews, J. B.R., Maycock, T.K., Waterfield, T., Yelekçi, O., Yu, R., Zhou, B. (Eds.), Climate Change 2021: The Physical Science Basis. Contribution of Working Group I to the Sixth Assessment Report of the Intergovernmental Panel on Climate Change. Cambridge University Press, Cambridge, United Kingdom and New York, NY, USA, pp. 1055–1210. https://doi.org/10.1017/9781009157896.010.

Eade, R., Stephenson, D.B., Scaife, A.A., Smith, D.M., 2022. Quantifying the rarity of extreme multidecadal trends: how unusual was the late twentieth century trend in the North Atlantic Oscillation? Climate Dynam. 58, 1555–1568. https://doi.org/10.1007/s00382-021-05978-4.

Ebel, B.A., Mirus, B.B., Heppner, C.S., VanderKwaak, J.E., Loague, K., 2009. First-order exchange coefficient coupling for simulating surface water–groundwater interactions: parameter sensitivity and consistency with a physics-based approach. Hydrol. Process. 23, 1949–1959. https://doi.org/10.1002/hyp.7279.

El Janyani, S., Massei, N., Dupont, J.-P., Fournier, M., Dörfliger, N., 2012. Hydrological responses of the chalk aquifer to the regional climatic signal. J. Hydrol. 464–465, 485–493. https://doi.org/10.1016/j.jhydrol.2012.07.040.

El Janyani, S., Dupont, J.P., Massei, N., Slimani, S., Dörfliger, N., 2014. Hydrological role of karst in the Chalk aquifer of Upper Normandy, France. Hydrgeol. J. 22, 663–677. https://doi.org/10.1007/s10040-013-1083-z.

Eyring, V., Bony, S., Meehl, G.A., Senior, C.A., Stevens, B., Stouffer, R.J., Taylor, K.E., 2016. Overview of the coupled model intercomparison project phase 6 (CMIP6) experimental design and organization. Geosci. Model Dev. 9 (5), 1937–1958. https://doi.org/10.5194/gmd-9-1937-2016.

Fatichi, S., Rimkus, S., Burlando, P., Bordoy, R., 2014. Does internal climate variability overwhelm climate change signals in streamflow? The upper Po and Rhone basin case studies. Sci. Total Environ. 493, 1171–1182. https://doi.org/10.1016/j.scitotenv.2013.12.014.

Flipo, N., Even, S., Poulin, M., Théry, S., Ledoux, E., 2007. Modeling nitrate fluxes at the catchment scale using the integrated tool CAWAQS. Sci. Total Environ. Human activity and material fluxes in a regional river basin: the Seine River watershed 375, 69–79. https://doi.org/10.1016/j.scitotenv.2006.12.016.

Flipo, N., Mouhri, A., Labarthe, B., Biancamaria, S., Rivière, A., Weill, P., 2014. Continental hydrosystem modelling: the concept of nested stream–aquifer interfaces. Hydrol. Earth Syst. Sci. 18, 3121–3149. https://doi.org/10.5194/hess-18-3121-2014.

Flipo, N., Lestel, L., Labadie, P., Meybeck, M., Garnier, J., 2021a. Trajectories of the Seine River Basin. In: Flipo, N., Labadie, P., Lestel, L. (Eds.), The Seine River Basin. Handbook of Environmental Chemistry, 90. Springer International Publishing, Cham, pp. 1–28. https://doi.org/10.1007/698_2019_437.

Flipo, N., Gallois, N., Labarthe, B., Baratelli, F., Viennot, P., Schuite, J., Rivière, A., Bonnet, R., Boé, J., 2021b. Pluri-annual water budget on the Seine Basin: Past, current and future trends. In: Flipo, N., Labadie, P., Lestel, L. (Eds.), The Seine River Basin. Handbook of Environmental Chemistry, 90. Springer International Publishing, Cham, pp. 59–89. https://doi.org/10.1007/698_2019_392.

Flipo, N., Gallois, N., Schuite, J., 2023. Regional coupled surface-subsurface hydrological model fitting based on a spatially distributed minimalist reduction of frequency-domain discharge data. Geosci. Model Dev. 16, 353–381. https://doi.org/10.5194/gmd-16-353-2023.

Fossa, M., Dieppois, B., Massei, N., Fournier, M., Laignel, B., Vidal, J.-P., 2021. Spatiotemporal and cross-scale interactions in hydroclimate variability: a case-study in France. Hydrol. Earth Syst. Sci. 25, 5683–5702. https://doi.org/10.5194/hess-25-5683-2021.

Girard, G., Ledoux, E., Villeneuve, J.-P., 1980. An integrated rainfall, surface and underground runoff model. La Houille Blanche 4 (5), 315–320.

Giuntoli, I., Renard, B., Vidal, J.-P., Bard, A., 2013. Low flows in France and their relationship to large-scale climate indices. J. Hydrol. 482, 105–118. https://doi.org/10.1016/j.jhydrol.2012.12.038.

Gu, L., Chen, J., Xu, C.-Y., Kim, J.-S., Chen, H., Xia, J., Zhang, L., 2019. The contribution of internal climate variability to climate change impacts on droughts. Sci. Total Environ. 684, 229–246. https://doi.org/10.1016/j.scitotenv.2019.05.345.

Gudmundsson, L., Tallaksen, L.M., Stahl, K., Fleig, A.K., 2011. Low-frequency variability of European runoff. Hydrol. Earth Syst. Sci. 15, 2853–2869. https://doi.org/10.5194/hess-15-2853-2011.

Haaf, E., Giese, M., Heudorfer, B., Stahl, K., Barthel, R., 2020. Physiographic and climatic controls on regional groundwater dynamics. Water Resour. Res. 56, e2019WR026545. https://doi.org/10.1029/2019WR026545.

Habets, F., Gascoin, S., Korkmaz, S., Thiéry, D., Zribi, M., Amraoui, N., Carli, M., Ducharne, A., Leblois, E., Ledoux, E., Martin, E., Noilhan, J., Ottlé, C., Viennot, P., 2010. Multi-model comparison of a major flood in the groundwater-fed basin of the Somme River (France). Hydrol. Earth Syst. Sci. 14, 99–117. https://doi.org/10.5194/hess-14-99-2010.

Hannaford, J., Buys, G., Stahl, K., Tallaksen, L.M., 2013. The influence of decadal-scale variability on trends in long European streamflow records. Hydrol. Earth Syst. Sci. 17, 2717–2733. https://doi.org/10.5194/hess-17-2717-2013.

He, C., Li, T., 2019. Does global warming amplify interannual climate variability? Climate Dynam. 52, 2667–2684. https://doi.org/10.1007/s00382-018-4286-0.

Holman, I.P., Rivas-Casado, M., Bloomfield, J.P., Gurdak, J.J., 2011. Identifying non-stationary groundwater level response to North Atlantic Ocean-atmosphere teleconnection patterns using wavelet coherence. Hydrgeol. J. 19, 1269. https://doi.org/10.1007/s10040-011-0755-9.

IPCC, 2021. Climate Change 2021: The Physical Science Basis. Contribution of Working Group I to the Sixth Assessment Report of the Intergovernmental Panel on Climate Change. Cambridge University Press, Cambridge, UK and New York, NY, USA.

Ledoux, E., Girard, G., Villeneuve, J.P., 1984. Proposition d'un modèle couplé pour la simulation conjointe des écoulements de surface et des écoulements souterrains sur un bassin hydrologique. La Houille Blanche 1-2, 101–120. https://doi.org/10.1051/lhb/1984005.

Ledoux, E., Girard, G., Marsily, G., Villeneuve, J.P., Deschenes, J., 1989. Spatially distributed modeling: conceptual approach, coupling surface water and groundwater. In: Morel-Seytoux, H.J. (Ed.), Unsaturated Flow in Hydrologic Modeling. Springer, Netherlands, Dordrecht, pp. 435–454. https://doi.org/10.1007/978-94-009-2352-2_16.

Lenton, T.M., Held, H., Kriegler, E., Hall, J.W., Lucht, W., Rahmstorf, S., Schellnhuber, H. J., 2008. Tipping elements in the Earth's climate system. P. Natl. Acad. Sci. USA 105, 1786–1793. https://doi.org/10.1073/pnas.0705414105.

Liesch, T., Wunsch, A., 2019. Aquifer responses to long-term climatic periodicities. J. Hydrol. 572, 226–242. https://doi.org/10.1016/j.jhydrol.2019.02.060.

Lorenzo-Lacruz, J., Morán-Tejeda, E., Vicente-Serrano, S.M., Hannaford, J., García, C., Peña-Angulo, D., Murphy, C., 2022. Streamflow frequency changes across western Europe and interactions with North Atlantic atmospheric circulation patterns. Global Planet. Change 212, 103797. https://doi.org/10.1016/j.gloplacha.2022.103797.

Machard de Gramont, H., Mardhel, V., 2006. Atlas des remontées de nappes en France métropolitaine, BRGM/RP-54414-FR. BRGM (105 pp.). http://infoterre.brgm.fr/rapports/RP-54414-FR.pdf.

Maréchal, J.-C., Rouillard, J., 2020. Groundwater in France: resources, use and management issues. In: Rinaudo, J.-D., Holley, C., Barnett, S., Montginoul, M. (Eds.), Sustainable Groundwater Management, Global Issues in Water Policy. Springer International Publishing, Cham, pp. 17–45. https://doi.org/10.1007/978-3-030-32766-8_2.

Martel, J.-L., Mailhot, A., Brissette, F., Caya, D., 2018. Role of natural climate variability in the detection of anthropogenic climate change signal for mean and extreme precipitation at local and regional scales. J. Climate 31, 4241–4263. https://doi.org/10.1175/JCLI-D-17-0282.1.

Massei, N., Fournier, M., 2012. Assessing the expression of large-scale climatic fluctuations in the hydrological variability of daily Seine river flow (France) between 1950 and 2008 using Hilbert–Huang Transform. J. Hydrol. 448–449, 119–128. doi: https://doi.org/10.1016/j.jhydrol.2012.04.052.

Massei, N., Durand, A., Deloffre, J., Dupont, J.P., Valdes, D., Laignel, B., 2007. Investigating possible links between the North Atlantic Oscillation and rainfall variability in northwestern France over the past 35 years. J. Geophys. Res. Atmos. 112, D09121. https://doi.org/10.1029/2005JD007000.

Massei, N., Laignel, B., Deloffre, J., Mesquita, J., Motelay, A., Lafite, R., Durand, A., 2010. Long-term hydrological changes of the Seine River flow (France) and their relation to the North Atlantic Oscillation over the period 1950–2008. Int. J. Climatol. 30, 2146–2154. https://doi.org/10.1002/joc.2022.

Massei, N., Dieppois, B., Hannah, D.M., Lavers, D.A., Fossa, M., Laignel, B., Debret, M., 2017. Multi-time-scale hydroclimate dynamics of a regional watershed and links to large-scale atmospheric circulation: application to the Seine river catchment. France. J. Hydrol. 546, 262–275. https://doi.org/10.1016/j.jhydrol.2017.01.008.

Matti, B., Dahlke, H.E., Dieppois, B., Lawler, D.M., Lyon, S.W., 2017. Flood seasonality across Scandinavia—evidence of a shifting hydrograph? Hydrol. Process. 31, 4354–4370. https://doi.org/10.1002/hyp.11365.

McCallum, J.L., Crosbie, R.S., Walker, G.R., Dawes, W.R., 2010. Impacts of climate change on groundwater in Australia: a sensitivity analysis of recharge. Hydrgeol. J. 18, 1625–1638. https://doi.org/10.1007/s10040-010-0624-y.

McMahon, T.A., Peel, M.C., Lowe, L., Srikanthan, R., McVicar, T.R., 2013. Estimating actual, potential, reference crop and pan evaporation using standard meteorological data: a pragmatic synthesis. Hydrol. Earth Syst. Sci. 17, 1331–1363. https://doi.org/10.5194/hess-17-1331-2013.

Neves, M.C., Jerez, S., Trigo, R.M., 2019. The response of piezometric levels in Portugal to NAO, EA, and SCAND climate patterns. J. Hydrol. 568, 1105–1117. https://doi.org/10.1016/j.jhydrol.2018.11.054.

Newcomer, M.E., Hubbard, S.S., Fleckenstein, J.H., Maier, U., Schmidt, C., Thullner, M., Ulrich, C., Flipo, N., Rubin, Y., 2016. Simulating bioclogging effects on dynamic riverbed permeability and infiltration. Water Resour. Res. 52, 2883–2900. https://doi.org/10.1002/2015WR018351.

O'Neill, M.M.F., Tijerina, D.T., Condon, L.E., Maxwell, R.M., 2021. Assessment of the ParFlow–CLM CONUS 1.0 integrated hydrologic model: evaluation of hyper-resolution water balance components across the contiguous United States. Geosci. Model Dev. 14, 7223–7254. https://doi.org/10.5194/gmd-14-7223-2021.

Oudin, L., Hervieu, F., Michel, C., Perrin, C., Andréassian, V., Anctil, F., Loumagne, C., 2005. Which potential evapotranspiration input for a lumped rainfall–runoff model?: part 2—towards a simple and efficient potential evapotranspiration model for rainfall–runoff modelling. J. Hydrol. 303, 290–306. https://doi.org/10.1016/j.jhydrol.2004.08.026.

Peña-Angulo, D., Vicente-Serrano, S.M., Domínguez-Castro, F., Murphy, C., Reig, F., Tramblay, Y., Trigo, R.M., Luna, M.Y., Turco, M., Noguera, I., Aznárez-Balta, M., García-Herrera, R., Tomas-Burguera, M., Kenawy, A.E., 2020. Long-term precipitation in Southwestern Europe reveals no clear trend attributable to anthropogenic forcing. Environ. Res. Lett. 15, 094070. https://doi.org/10.1088/1748-9326/ab9c4f.

Percival, D.B., Walden, A.T., 2000. Wavelet Methods for Time Series Analysis. Cambridge University Press, Cambridge.

Perrin, C., Michel, C., Andréassian, V., 2003. Improvement of a parsimonious model for streamflow simulation. J. Hydrol. 279, 275–289. https://doi.org/10.1016/S0022-1694(03)00225-7.

Qasmi, S., Cassou, C., Boé, J., 2017. Teleconnection between Atlantic multidecadal variability and European temperature: diversity and evaluation of the coupled model Intercomparison project phase 5 models. Geophys. Res. Lett. 44, 11,140-11,149. doi: https://doi.org/10.1002/2017GL074886.

Quintana-Seguí, P., Moigne, P.L., Durand, Y., Martin, E., Habets, F., Baillon, M., Canellas, C., Franchisteguy, L., Morel, S., 2008. Analysis of near-surface atmospheric variables: validation of the SAFRAN analysis over France. J. Appl. Meteorol. Climatol. 47, 92–107. https://doi.org/10.1175/2007JAMC1636.1.

Rivière, A., Gonçalvès, J., Jost, A., Font, M., 2014. Experimental and numerical assessment of transient stream–aquifer exchange during disconnection. J. Hydrol. 517, 574–583. https://doi.org/10.1016/j.jhydrol.2014.05.040.

Roux, J.C., 2006. Aquifères et eaux souterraines en France. BRGM Editions, p. 956p.

Rushton, K., 2007. Representation in regional models of saturated river–aquifer interaction for gaining/losing rivers. J. Hydrol. 334, 262–281. https://doi.org/10.1016/j.jhydrol.2006.10.008.

Rust, W., Holman, I., Corstanje, R., Bloomfield, J., Cuthbert, M., 2018. A conceptual model for climatic teleconnection signal control on groundwater variability in Europe. Earth Sci. Rev. 177, 164–174. https://doi.org/10.1016/j.earscirev.2017.09.017.

Rust, W., Bloomfield, J.P., Cuthbert, M., Corstanje, R., Holman, I., 2022. The importance of non-stationary multiannual periodicities in the North Atlantic Oscillation index for forecasting water resource drought. Hydrol. Earth Syst. Sci. 26, 2449–2467. https://doi.org/10.5194/hess-26-2449-2022.

Saleh, F., Flipo, N., Habets, F., Ducharne, A., Oudin, L., Viennot, P., Ledoux, E., 2011. Modeling the impact of in-stream water level fluctuations on stream-aquifer interactions at the regional scale. J. Hydrol. 400, 490–500. https://doi.org/10.1016/j.jhydrol.2011.02.001.

Sauquet, E., Evin, G., Siauve, S., Bornancin-Plantier, A., Jacquin, N., Arnaud, P., Bérel, M., Bernus, S., Bonneau, J., Branger, F., Caballero, Y., Colléoni, F., Collet, L., Corre, L., Drouin, A., Ducharne, A., Fournier, M., Gailhard, J., Habets, F., Hendrickx, F., Héraut, L., Hingray, B., Huang, P., Jaouen, T., Jeantet, A., Lanini, S., Le Lay, M., Loudin, S., Magand, C., Marson, P., Mimeau, L., Monteil, C., Munier, S., Perrin, C., Robin, Y., Rousset, F., Soubeyroux, J.-M., Strohmenger, L., Thirel, G., Tocquer, F., Tramblay, Y., Vergnes, J.-P., Vidal, J.-P., Vrac, M., 2024. Messages et enseignements du projet Explore2. Recherche Data Gouv V7. https://doi.org/10.57745/J3XIPW.

Schuite, J., Flipo, N., Massei, N., Rivière, A., Baratelli, F., 2019. Improving the spectral analysis of hydrological signals to efficiently constrain watershed properties. Water Resour. Res. 55, 4043–4065. https://doi.org/10.1029/2018WR024579.

Seguin, J.-J., Allier, D., Manceau, J.-C., 2019. Contribution d'un index piézométrique standardisé à l'analyse de l'impact des sécheresses sur les ressources en eau souterraines. Géologues 202, 43–48.

Sidibe, M., Dieppois, B., Eden, J., Mahé, G., Paturel, J.-E., Amoussou, E., Anifowose, B., Lawler, D., 2019. Interannual to multi-decadal streamflow variability in West and Central Africa: interactions with catchment properties and large-scale climate variability. Global Planet. Change 177, 141–156. https://doi.org/10.1016/j.gloplacha.2019.04.003.

Slimani, S., Massei, N., Mesquita, J., Valdés, D., Fournier, M., Laignel, B., Dupont, J.-P., 2009. Combined climatic and geological forcings on the spatio-temporal variability of piezometric levels in the chalk aquifer of Upper Normandy (France) at pluridecennal scale. Hydrgeol. J. 17, 1823. https://doi.org/10.1007/s10040-009-0488-1.

Starck, J.L., Farrens, S., Tersenov, A., Leterme, H., Lanusse, F., 2020. CosmoStat. https://github.com/CosmoStat/cosmostat. (Accessed 16 September 2024).

Starck, J.-L., Fadili, J., Murtagh, F., 2007. The undecimated wavelet decomposition and its reconstruction. IEEE Trans. Image Process. 16, 297–309. https://doi.org/10.1109/TIP.2006.887733.

Terray, L., Boé, J., 2013. Quantifying 21st-century France climate change and related uncertainties. C. R. Geosci. 345, 136–149. https://doi.org/10.1016/j.crte.2013.02.003.

Velasco, E.M., Gurdak, J.J., Dickinson, J.E., Ferré, T.P.A., Corona, C.R., 2017. Interannual to multidecadal climate forcings on groundwater resources of the U.S. West Coast. J. Hydrol.: Regional Studies. Water, energy, and food nexus in the Asia-Pacific region 11, 250–265. https://doi.org/10.1016/j.ejrh.2015.11.018.

Vergnes, J.-P., Caballero, Y., Lanini, S., 2023. Assessing climate change impact on French groundwater resources using a spatially distributed hydrogeological model. Hydrol. Sci. J. 68 (2), 209–227. https://doi.org/10.1080/02626667.2022.2150553.

Vidal, J.-P., Martin, E., Franchistéguy, L., Baillon, M., Soubeyroux, J.-M., 2010. A 50-year high-resolution atmospheric reanalysis over France with the Safran system. Int. J. Climatol. 30, 1627–1644. https://doi.org/10.1002/joc.2003.

Winckel, A., Ollagnier, S., Gabillard, S., 2022. Managing groundwater resources using a national reference database: the French ADES concept. SN Appl. Sci 4, 217. https://doi.org/10.1007/s42452-022-05082-0.

Wood, E., Roundy, J., Troy, T., van Beek, L., Bierkens, M., Blyth, E., de Roo, A., Döll, P., Ek, M., Famiglietti, J., Gochis, D., van de Giesen, N., Houser, P., Jaffé, P., Kollet, S., Lehner, B., Lettenmaier, D., Peters-Lidard, C., Sivapalan, M., Sheffield, J., Wade, A., Whitehead, P., 2011. Hyperresolution global land surface modeling: meeting a grand challenge for monitoring Earth's terrestrial water. Water Resour. Res. 47, W05301. https://doi.org/10.1029/2010WR010090.

Wunsch, A., Liesch, T., Broda, S., 2022. Deep learning shows declining groundwater levels in Germany until 2100 due to climate change. Nat. Commun. 13, 1221. https://doi.org/10.1038/s41467-022-28770-2.

Xanke, J., Liesch, T., 2022. Quantification and possible causes of declining groundwater resources in the Euro-Mediterranean region from 2003 to 2020. Hydrgeol. J. 30, 379–400. https://doi.org/10.1007/s10040-021-02448-3.